$yN$ -39 $43499$

# Element Library for Three-Dimensional Stress Analysis by the Integrated Force Method

Igor Kaljević, Surya N. Patnaik, and Dale A. Hopkins

APRIL 1996

National Aeronautics and
Space Administration

# Element Library for Three-Dimensional Stress Analysis by the Integrated Force Method

Igor Kaljević and Surya N. Patnaik
*Ohio Aerospace Institute*
*Cleveland, Ohio*

Dale A. Hopkins
*Lewis Research Center*
*Cleveland, Ohio*

# ELEMENT LIBRARY FOR THREE-DIMENSIONAL STRESS ANALYSIS BY THE INTEGRATED FORCE METHOD

Igor Kaljević and Surya N. Patnaik
Ohio Aerospace Institute
Cleveland, Ohio 44142

and

Dale A. Hopkins
National Aeronautics and Space Administration
Lewis Research Center
Cleveland, Ohio 44135

## Summary

The Integrated Force Method, a recently developed method for analyzing structures, is extended in this paper to three-dimensional structural analysis. First, a general formulation is developed to generate the stress interpolation matrix in terms of complete polynomials of the required order. The formulation is based on definitions of the stress tensor components in terms of stress functions. The stress functions are written as complete polynomials and substituted into expressions for stress components. Then elimination of the dependent coefficients leaves the stress components expressed as complete polynomials whose coefficients are defined as generalized independent forces. Such derived components of the stress tensor identically satisfy homogenous Navier equations of equilibrium. The resulting element matrices are invariant with respect to coordinate transformation and are free of spurious zero-energy modes. The formulation provides a rational way to calculate the exact number of independent forces necessary to arrive at an approximation of the required order for complete polynomials. The influence of reducing the number of independent forces on the accuracy of the response is also analyzed. The stress fields derived are used to develop a comprehensive finite element library for three-dimensional structural analysis by the Integrated Force Method. Both tetrahedral- and hexahedral-shaped elements capable of modeling arbitrary geometric configurations are developed. A number of examples with known analytical solutions are solved by using the developments presented herein. The results are in good agreement with the analytical solutions. The responses obtained with the Integrated Force Method are also compared with those generated by the standard displacement method. In most cases, the performance of the Integrated Force Method is better overall.

## Introduction

The finite element method has become the preferred tool for analyzing a wide variety of physical problems. The advantages of the finite element method over other numerical techniques, such as the finite difference method and the boundary element method, include the efficient and accurate modeling of domains with arbitrary geometric configurations and varying material parameters and the capability to analyze problems with both material and geometric nonlinearities. Two distinct finite element formulations, based on the primary unknown variables used in the analysis, have been developed for analyzing problems in structural mechanics, namely, the displacement method (refs. 1 to 3) and the standard force method (refs. 4 and 5). The displacement method has become prevalent in structural analysis because of its straightforward implementation and efficient use of computer resources. It has been implemented in all commercial finite element programs. Implementation of the standard force method, on the other hand, requires either a selection of redundant forces (ref. 4) or extensive manipulation of system matrices (refs. 5 to 7) in order to generate a system of equations for the unknown variables. Since these procedures could not easily be adapted for computer automation and since they lacked a physical interpretation, the standard force method met its demise.

Certain drawbacks of the displacement-based method have been observed in a number of applications, such as the bending of thin plates, the analysis of nearly incompressible materials, and the optimization of structures (refs. 7 to 11). In the displacement method, stresses are calculated indirectly by using displacement derivatives, which may introduce errors in stress predictions. Thus, there is a need to develop alternative finite element formulations to treat the aforementioned problems and to provide a means of comparison for other numerical methods.

A new force method formulation for analyzing structures (refs. 12 to 15), known as the Integrated Force Method, has been developed in recent years. In the Integrated Force Method all independent forces are treated as unknown variables that can be obtained by solving a system of equations consisting of equations of equilibrium and compatibility conditions. Compatibility conditions are derived in a procedure similar to the St. Venant procedure for continuous elasticity (ref. 16). Several classes of compatibility conditions have been identified, and a method for generating compatibility conditions has been developed (ref. 17). This method efficiently utilizes computer resources and produces a sparse and banded compatibility matrix. The Integrated Force Method has been successfully applied to static (ref. 12) and free vibration (ref. 18) analyses and to structural optimization (refs. 19 to 21). Initial comparisons with other finite element formulations have revealed the superiority of the Integrated Force Method in accuracy as well as in computer efficiency (ref. 22).

In the Integrated Force Method, two sets of relations are established: the equilibrium relations and the deformation-force relations. These relations are first derived on the element level through equilibrium and flexibility matrices, respectively (ref. 23). Next, appropriate assembly techniques are used (ref. 14) to generate systems of equations for the entire structure. In order to generate element matrices, approximations of both displacement and stress fields have to be defined. Here, these approximations are performed independently; the displacement components within an element are approximated in terms of element nodal displacements, whereas the components of the stress tensor are proposed in terms of a set of independent generalized forces. Although the interpolation of the displacement field is straightforward and does not significantly influence the accuracy of calculations in the Integrated Force Method, the correct approximation of the stress field is of utmost importance for both accuracy and computer efficiency. Stress field interpolations were previously studied in applications of the hybrid method (refs. 8, 9, and 24 to 26). Spilker and Singh (ref. 9) derived two stress field interpolations for a 20-node isoparametric element; Pian and Sumihara (ref. 25) used nondimensional coordinates; and Pian et al. (ref. 26) explored the possibility of achieving the minimum number of independent forces (ref. 27) while relaxing some requirements for stress fields.

The Integrated Force Method is extended in this paper to three-dimensional structural analysis. To this end an extensive library of finite elements capable of analyzing domains with arbitrary geometric configurations is developed. First, a general formulation is developed to generate the stress interpolation functions in terms of complete polynomials of the required order. The formulation is based on definitions of stress components in terms of stress functions. The stress functions are written in terms of complete polynomials of a certain order with coefficients that are arbitrary constants. Expressions for stresses are obtained next by substituting expressions for stress functions. Then the linearly dependent constants are eliminated, thereby yielding final stresses expressed in terms of complete polynomials whose coefficients are now element-generalized independent forces. Such derived stress fields identically satisfy Navier's equations of equilibrium. The element matrices generated with these polynomials are invariant with respect to coordinate transformation and are free of spurious zero-energy modes for arbitrary orientation of the element local coordinate system. This formulation also provides a rational way to calculate the exact number of independent forces for an approximation with complete polynomials of the required order. Representing the stress field with complete polynomials may result in a significantly larger number of independent forces than the minimum number determined by rigid body modes considerations. This paper discusses the reduction in the number of independent forces and some guidelines for determining the stress fields properties necessary to achieving good approximations.

The stress fields derived by using the developments presented herein are used to develop a comprehensive finite element library for three-dimensional structural analysis by the Integrated Force Method. Both tetrahedral- and hexahedral-shaped elements capable of modeling arbitrary configurations are considered. Stress fields that were derived earlier for hybrid elements (refs. 5 and 9) and given in terms of reduced polynomials are also implemented to study the effects of reduction on accuracy.

To establish their validity and accuracy, the elements presented here are used to solve a number of example problems with known analytical solutions. These results are compared to those obtained with the standard displacement method to assess the relative performances of the two methods. The expressions for stress fields are given in appendix A, and the symbols used are defined in appendix B.

## Basic Equations of the Integrated Force Method

The governing equations of the Integrated Force Method are briefly reviewed here to ensure completeness and to introduce the notation. The derivation of these equations and a description of the method are detailed in references 12 to 14. Expressions for element matrices are derived in reference 23.

In an analysis by the Integrated Force Method, a continuous object under consideration is discretized into a number of finite elements. Within each finite element the displacement and stress fields are approximated in terms of two sets of independent variables as

$$\{u\} = [N]\{U_e\} \qquad (1)$$

2

$$\{\sigma\} = [Y]\{F_e\} \qquad (2)$$

where $\{u\}^T = \{u \; v \; w\}$ is the displacement vector with components $u$, $v$, and $w$ along the global coordinate axes $Ox$, $Oy$, and $Oz$, respectively; $\{U_e\}$ is the vector of displacements at element nodes resulting from the finite element discretization; $\{\sigma\}^T = \{\sigma_x \; \sigma_y \; \sigma_z \; \tau_{xy} \; \tau_{yz} \; \tau_{zx}\}$ is the vector of stress components; $\{F_e\}$ is the vector of element independent generalized forces; $[N]$ is the matrix of displacement interpolation functions; and $[Y]$ is the stress interpolation matrix. Such a finite element discretization results in a total of $N_t$ displacement degrees of freedom and $m$ independent forces. Two sets of relations can be written for each element of the discretization:

(a) the equations of equilibrium

$$\{P_e\} = [B_e]\{F_e\} \qquad (3)$$

and

(b) the deformation-force relation

$$\{\beta_e\} = [G_e]\{F_e\} \qquad (4)$$

where $\{P_e\}$ is the equivalent nodal load vector of the element; $\{\beta_e\}$ is the vector of element deformations corresponding to the forces $\{F_e\}$; and $[B_e]$ and $[G_e]$ are the element equilibrium and flexibility matrices, respectively, which are calculated (ref. 23) as

$$[B_e] = \int_V [Z]^T[Y]dV \qquad (5a)$$

$$[G_e] = \int_V [Y]^T[D][Y]dV \qquad (5b)$$

In equations (5), $[D]$ is the compliance matrix of the material, and $[Z] = [L][N]$, where $[L]$ is the matrix of differential operators that defines the strain-displacement relationship. For all free nodes, equation (3) can be written to generate a system of $n$ equations of equilibrium:

$$[B_p]\{F\} = \{P\} \qquad (6)$$

Here $[B_p]$ is the $(m \times n)$ system equilibrium matrix; $\{F\}$ is the system vector of independent forces of dimension $n$; and $\{P\}$ is the $m$-component vector of equivalent nodal loads. For a general problem, $m \geq n$, and the system given in equation (6) is indeterminate and not sufficient to calculate the independent forces. This system of equations (eq. (6)) must be augmented by a set of $r = m - n$ compatibility conditions (ref. 17) which, for the case of mechanical loads, have the form

$$[C][G]\{F\} = \{0\} \qquad (7)$$

where $[G]$ is the system flexibility matrix and $[C]$ is the compatibility matrix. The procedures for automatically generating the compatibility matrix are given in reference 17. Equations (6) and (7) provide the necessary and sufficient number of equations to calculate the vector of independent forces $\{F\}$. The resulting system of equations may be written in a compact form as

$$[S]\{F\} = \{P^*\} \qquad (8)$$

where

$$[S] = \begin{bmatrix} [B_p] \\ [C][G] \end{bmatrix} \quad \text{and} \quad \{P^*\} = \begin{Bmatrix} \{P\} \\ \{0\} \end{Bmatrix} \qquad (9)$$

After the force vector is calculated from equation (8), the vectors of the unknown nodal displacements $\{U\}$ and the support reactions $\{R\}$ may be obtained as

$$\{U\} = [J] \; [G] \; \{F\} \qquad (10a)$$

$$\{R\} = [B_s] \; \{F\} \qquad (10b)$$

where $[J]$ is the $n \times m$ deformation matrix that represents the top $m$ rows of the transpose of the matrix $[S]^{-1}$; and $[B_s]$ is the portion of the system equilibrium matrix that corresponds to nodes with prescribed displacement boundary conditions.

## Approximations of the Stress Field

Approximating the stress field within a finite element and generating the stress interpolation matrix $[Y]$ are discussed in this section. The stress interpolation matrix appears in definitions of both the equilibrium and flexibility matrices (see eqs. (5)). It is, therefore, necessary to properly devise the stress interpolation functions in order to obtain an accurate response. The required properties of stress interpolation polynomials, in the context of hybrid method applications, were discussed by Spilker et al. (refs. 8 and 9) and Pian et al. (ref. 26). They found that approximate stress fields should identically satisfy Navier's equations of equilibrium, that the stress components should be symmetric, and that the resulting element matrices should be invariant with respect to coordinate transformations and be free of spurious zero-energy modes. Spilker, Maskeri, and Kania (ref. 8) have shown that a necessary and sufficient

condition for element matrices to be invariant with respect to coordinate transformation is that stress fields be approximated in terms of complete polynomials. In reference 23, the same requirement was deduced for the Integrated Force Method finite elements. A formulation to derive stress interpolation functions as complete polynomials of arbitrary order is developed herein, and then the reduced stress fields are discussed.

## Stress Fields in Terms of Complete Polynomials

Stress interpolation functions in terms of complete polynomials of order $p - 2$, where $p \geq 2$ is an integer, are derived in this section. To this end, the stress functions $\Phi_k$, for $k = 1$, 2, 3, are proposed as complete polynomials of order $p$ such that

$$\Phi_k(x,y,z) = \sum_{i=0}^{p} \sum_{j=0}^{p-i} C_{i,j}^{(k)} x^i y^j z^{p-i-j} \qquad k = 1,2,3 \quad (11)$$

where $C_{i,j}^k$ for $i = 0, 1, ..., p$, and $j = 0, 1, ..., (p - i)$ are arbitrary coefficients, and $(x, y, z)$ denotes the position of a point within a finite element in the element local coordinate system. Local coordinate systems for various element shapes are depicted in figure 1. The expressions for stress components can be obtained from the definitions of stress functions (ref. 28) as

$$\sigma_x = \frac{\partial^2 \Phi_2}{\partial z^2} + \frac{\partial^2 \Phi_3}{\partial y^2} = \sum_{i=0}^{p-2} \sum_{j=0}^{p-i-2} \left[ C_{i,j}^{(2)}(p-i-j)(p-i-j-1) \right.$$

$$\left. + C_{i,j+2}^{(3)}(j+1)(j+2) \right] x^i y^j z^{p-i-j-2} \quad (12a)$$

$$\sigma_y = \frac{\partial^2 \Phi_3}{\partial x^2} + \frac{\partial^2 \Phi_1}{\partial z^2} = \sum_{i=0}^{p-2} \sum_{j=0}^{p-i-2} \left[ C_{i+2,j}^{(3)}(i+1)(i+2) \right.$$

$$\left. + C_{i,j}^{(1)}(p-i-j)(p-i-j-1) \right] x^i y^j z^{p-i-j-2} \quad (12b)$$

$$\sigma_z = \frac{\partial^2 \Phi_1}{\partial y^2} + \frac{\partial^2 \Phi_2}{\partial x^2} = \sum_{i=0}^{p-2} \sum_{j=0}^{p-i-2} \left[ C_{i,j+2}^{(1)}(j+1)(j+2) \right.$$

$$\left. + C_{i+1,j}^{(2)}(i+1)(i+2) \right] x^i y^j z^{p-i-j-2} \quad (12c)$$

| Shape | Nodes | Forces | Name | Number of integration points |
|---|---|---|---|---|
|  | 4 | 6 | THD04_06 | 1 |
| | | 18 | THD04_18 | 5 |
| | | 21 | THD04_21 | 5 |
|  | 8 | 18 | HEX08_18 | 3x3x3 |
| | | 33 | HEX08_33 | 3x3x3 |
| | | 48 | HEX08_48 | 3x3x3 |
|  | 10 | 36 | THD10_36 | 11 |
| | | 39 | THD10_39 | 11 |
| | | 48 | THD10_48 | 11 |
|  | 20 | 57 | HEX20_57 | 4x4x4 |
| | | 60 | HEX20_60 | 4x4x4 |
| | | 90 | HEX20_90 | 4x4x4 |

Figure 1.—Finite elements for three-dimensional analysis. (Numerical integration for THD elements use ref. 1; likewise, HEX elements use ref. 29 for quadrature.)

$$\tau_{xy} = \frac{\partial^2 \Phi_3}{\partial x \partial y} = -\sum_{i=0}^{p-2} \sum_{j=0}^{p-i-2} C_{i+1,j+1}^{(3)}(i+1)(j+1)$$

$$\times x^i y^j z^{p-i-j-2} \quad (12d)$$

$$\tau_{yz} = \frac{\partial^2 \Phi_1}{\partial y \partial z} = -\sum_{i=0}^{p-2} \sum_{j=0}^{p-i-2} C_{i,j+1}^{(1)}(j+1)(p-i-j-1)$$

$$\times x^i y^j z^{p-i-j-2} \quad (12e)$$

$$\tau_{zx} = \frac{\partial^2 \Phi_2}{\partial z \partial x} = -\sum_{i=0}^{p-2} \sum_{j=0}^{p-i-2} C_{i+1,j}^{(2)}(i+1)(p-i-j-1)$$

$$\times x^i y^j z^{p-i-j-2} \quad (12f)$$

Equations (12) can now be rewritten as

$$\sigma_x = \sum_{i=0}^{p-2} \sum_{j=0}^{p-i-2} \tilde{F}_{i \times (p-i-2)+j} \, x^i y^j z^{p-i-j-2} \quad (13a)$$

$$\sigma_y = \sum_{i=0}^{p-2} \sum_{j=0}^{p-i-2} \tilde{F}_{P+i \times (p-i-2)+j} \, x^i y^j z^{p-i-j-2} \quad (13b)$$

$$\sigma_z = \sum_{i=0}^{p-2} \sum_{j=0}^{p-i-2} \tilde{F}_{2P+i\times(p-i-2)+j}\, x^i y^j z^{p-i-j-2} \qquad (13c)$$

$$\tau_{xy} = \sum_{i=0}^{p-2} \sum_{j=0}^{p-i-2} \tilde{F}_{3P+i\times(p-i-2)+j}\, x^i y^j z^{p-i-j-2} \qquad (13d)$$

$$\tau_{yz} = \sum_{i=0}^{p-2} \sum_{j=0}^{p-i-2} \tilde{F}_{4P+i\times(p-i-2)+j}\, x^i y^j z^{p-i-j-2} \qquad (13e)$$

$$\tau_{zx} = \sum_{i=0}^{p-2} \sum_{j=0}^{p-i-2} \tilde{F}_{5P+i\times(p-i-2)+j}\, x^i y^j z^{p-i-j-2} \qquad (13f)$$

where $P = (1/2)p(p-1)$, and the coefficients $\tilde{F}_q$, for $q = 1$, 2, ..., $6P$, denote element-generalized forces. Generalized forces $\tilde{F}_q$ are expressed in terms of $C^{(k)}_{i,j}$ as

$$\tilde{F}_q = \phi_q\!\left(C^{(k)}_{i,j}\right) \quad \text{for } q = 1,2,...,6P \qquad (14)$$

where $\phi_q$ represents the linear functions of constants $C^{(k)}_{i,j}$. From equation (14) we can see that $3p(p-1)$ forces $\tilde{F}_q$ are expressed in terms of $(3/2)(p-1)(p+4)$ constants $C^{(k)}_{i,j}$. Eliminating all dependent quantities from equations (13) yields final expressions for stress polynomials in terms of $Q = (3/2) \times (p-1)(p+2)$ independent generalized forces $\tilde{F}_q$, for $q = 1$, 2, ..., $Q$. Such generated stress fields identically satisfy the equations of equilibrium. The element matrices generated by using these stress fields are invariant with respect to coordinate transformation and are free of spurious zero-energy modes.

A general procedure for deriving the stress interpolation matrix in terms of complete polynomials can be illustrated through the derivation of linear terms. For this case, the stress functions $\Phi_k$, for $k = 1, 2, 3$, are written as complete third-order polynomials,

$$\Phi_k(x,y,z) = C^{(k)}_{0,0}z^3 + C^{(k)}_{0,1}yz^2 + C^{(k)}_{0,2}y^2z + C^{(k)}_{0,3}y^3 + C^{(k)}_{1,0}z^2x$$

$$+ C^{(k)}_{1,1}xyz + C^{(k)}_{1,2}xy^2 + C^{(k)}_{2,0}x^2z + C^{(k)}_{2,1}x^2y + C^{(k)}_{3,0}x^3 \qquad (15)$$

where $C^{(k)}_{i,j}$, for $i = 0, 1, 2, 3$, and $j = 0, 1, ..., (3-i)$ are coefficients of the cubic polynomials. From the definitions of stress

components in terms of stress functions, the expressions for stresses can be obtained as

$$\sigma_x = \left(2C^{(2)}_{1,0} + 2C^{(3)}_{1,2}\right)x + \left(2C^{(2)}_{0,1} + 2C^{(3)}_{0,3}\right)y$$

$$+ \left(6C^{(2)}_{0,0} + 2C^{(3)}_{0,2}\right)z \qquad (16a)$$

$$\sigma_y = \left(6C^{(3)}_{3,0} + 2C^{(1)}_{1,0}\right)x + \left(2C^{(3)}_{2,1} + 2C^{(1)}_{0,1}\right)y$$

$$+ \left(2C^{(3)}_{2,0} + 6C^{(1)}_{0,0}\right)z \qquad (16b)$$

$$\sigma_z = \left(2C^{(1)}_{1,2} + 2C^{(2)}_{3,0}\right)x + \left(6C^{(1)}_{0,3} + 2C^{(2)}_{2,1}\right)y$$

$$+ \left(2C^{(1)}_{0,2} + 2C^{(2)}_{2,0}\right)z \qquad (16c)$$

$$\tau_{xy} = -\left(2C^{(3)}_{2,1}x + 2C^{(3)}_{1,2}y + C^{(3)}_{1,1}z\right) \qquad (16d)$$

$$\tau_{yz} = -\left(C^{(1)}_{1,1}x + 2C^{(1)}_{0,2}y + 2C^{(1)}_{0,1}z\right) \qquad (16e)$$

$$\tau_{zx} = -\left(2C^{(2)}_{2,0}x + C^{(2)}_{1,1}y + 2C^{(2)}_{1,0}z\right) \qquad (16f)$$

Equations (16) may be written in terms of element forces $\tilde{F}_i$ as

$$\sigma_x = \tilde{F}_1 x + \tilde{F}_2 y + \tilde{F}_3 z \qquad (17a)$$

$$\sigma_y = \tilde{F}_4 x + \tilde{F}_5 y + \tilde{F}_6 z \qquad (17b)$$

$$\sigma_z = \tilde{F}_7 x + \tilde{F}_8 y + \tilde{F}_9 z \qquad (17c)$$

$$\tau_{xy} = \tilde{F}_{10} x + \tilde{F}_{11} y + \tilde{F}_{12} z \qquad (17d)$$

$$\tau_{yz} = \tilde{F}_{13} x + \tilde{F}_{14} y + \tilde{F}_{15} z \qquad (17e)$$

$$\tau_{zx} = \tilde{F}_{16} x + \tilde{F}_{17} y + \tilde{F}_{18} z \qquad (17f)$$

Expressions for forces $\tilde{F}_i$ in terms of coefficients $C^{(k)}_{i,j}$ can be obtained by comparing corresponding terms in equations (16) and (17). A careful examination of these expressions

5

reveals that not all forces $\tilde{F}_i$ are linearly independent. Three relationships exist:

$$\tilde{F}_1 + \tilde{F}_{11} + \tilde{F}_{18} = 0 \qquad (18a)$$

$$\tilde{F}_5 + \tilde{F}_{10} + \tilde{F}_{15} = 0 \qquad (18b)$$

$$\tilde{F}_9 + \tilde{F}_{14} + \tilde{F}_{16} = 0 \qquad (18c)$$

Eliminating forces $\tilde{F}_{11}$, $\tilde{F}_{15}$, and $\tilde{F}_{16}$ in equations (17) through use of equations (18) and renumbering yields the linear terms of the stress polynomials given in equations (A2) in appendix A. The terms of constant, quadratic, and cubic orders can be obtained by following a similar procedure; they are given in equations (A1), (A3), and (A4), respectively. The stress field representation in terms of complete polynomials of order $p$ can be obtained by combining the expressions for orders 0, 1,..., $p$. The interpolation in terms of complete cubic polynomials is given in equations (A5). The constant stress field is obtained by retaining the first six terms in equations (A5). For the linear interpolation, the first 21 terms are retained; for the quadratic interpolation, 48 terms are retained.

### Reduced Stress Fields

Stress interpolation with complete polynomials may result in a large number of independent forces for each element, which leads to a final system of equations that is quite large. This problem is particularly pronounced in three-dimensional analyses, where the difference between the number of independent forces in complete polynomials and the minimum required number calculated from the number of rigid body modes for a particular element (ref. 27) grows rapidly as the order of interpolation increases. An effort should therefore be made to reduce the number of independent forces in stress interpolation polynomials while preserving the accuracy and reliability of the resulting elements. Reduced stress fields were studied by a number of researchers (refs. 9 and 26) with the goal of devising stress interpolations containing the minimum number of independent forces. Such derived stress fields, however, may violate the requirements for accuracy stated earlier. There is no rational procedure available to uniquely derive stress fields with the minimum number of independent forces, and there is no proof that the resulting elements are free of spurious zero-energy modes. Moreover, in some problems these elements may fail unexpectedly. Therefore, reduced stress fields should be used with caution, and extensive numerical studies should be performed to verify the resulting elements. The guidelines suggested by Pian, Chen, and Kang (ref. 26) were followed in this study to derive the two reduced quadratic stress fields given in equations (A9) and (A10) and the reduced cubic stress field given in equations (A11). The

stress fields developed by Spilker and Singh (ref. 9) and Robinson (ref. 5) for hybrid finite elements were also implemented for comparison purposes.

## Finite Elements for Three-Dimensional Analysis

In this section, a comprehensive finite element library for three-dimensional analysis by the Integrated Force Method is presented. Both tetrahedral- and hexahedral-shaped elements capable of modeling domains with arbitrary configurations were generated. Two groups of elements were developed for each shape. In the first group, nodes were introduced only at the vertices, thereby producing four-node tetrahedrons and eight-node hexahedrons. In the second group, additional nodes were introduced on the element edges as well, thereby producing 10-node tetrahedrons and 20-node hexahedrons. The attributes of the elements of the library presented here are depicted in figure 1. The names given to these elements consist of three parts: the first three characters denote the element shape, two subsequent digits denote the number of element nodes, and the number following the underscore denotes the number of independent forces used in the stress interpolation. A local coordinate system $Oxyz$ for stress interpolation is defined such that the origin $O$ coincides with the element centroid, and the local axes $Ox$, $Oy$, and $Oz$ are parallel to the corresponding global axes. For all elements presented here, isoparametric functions (ref. 1) are used to interpolate the displacement fields. The characteristics of these elements are enumerated in the following sections.

### Four-Node Tetrahedral Elements: THD04_06, THD04_18, and THD04_21

Four-node tetrahedrons have 12 kinematic degrees of freedom and thus require at least 6 independent forces in their stress field description. The six independent forces define complete polynomials of order zero, that is, the constant stress field. This stress field was implemented for element THD04_06. Since element THD04_06 contains the minimum required number of independent forces, it is a statically determinate element (ref. 23). Higher order stress fields were also implemented to investigate the influence that the order of interpolation has on accuracy. The complete linear stress field was used for element THD04_21, and the 18-force stress field developed by Robinson (ref. 5), given in equations (A6), was used for element THD04_18.

### Eight-Node Hexahedral Elements: HEX08_18, HEX08_33, and HEX08_48

Eight-node hexahedral elements have 24 kinematic degrees of freedom and thus require at least 18 independent forces in

their stress field interpolation polynomials. Robinson's stress field, given in equations (A6), was implemented for element HEX08_18, which represents a statically determinate eight-node hexahedron. Let us consider the complete polynomials for eight-node hexahedrons. First-order polynomials with 21 independent forces satisfy the criterion for the minimum number of forces. The test for zero-energy modes (ref. 23) reveals, however, that the resulting element possesses three spurious zero-energy modes. This behavior confirms that displacement and stress fields within an element cannot be chosen arbitrarily, but should be compatible with the stress-strain relationships. In order to obtain an element with complete polynomials, the second order was employed for element HEX08_48. Since this element contains a significantly larger number of independent forces than necessary, a reduced stress field was obtained with 21 independent forces corresponding to complete linear polynomials, combined with a reduced quadratic field with 12 additional forces (given in eqs. (A8)). This stress field identically satisfies Navier's equations of equilibrium, and the resulting element does not possess spurious zero-energy modes.

### Ten-Node Tetrahedral Elements: THD10_36, THD10_39, and THD10_48

Ten-node elements possess 30 kinematic degrees of freedom and require 24 independent forces in stress interpolation polynomials. For this case, at least a second-order polynomial is required, and such an implementation was carried out for element THD10_48. Two reduced quadratic stress fields were also implemented. Both of these fields contain complete linear polynomials and a number of quadratic terms. The linear polynomials were combined with the quadratic terms given in equations (A9) to generate the stress fields used for element THD10_39, and with the quadratic terms given in equations (A10) to obtain the stress fields implemented for element THD10_36. Both of these fields identically satisfy the equations of equilibrium, and the resulting elements are free of spurious zero-energy modes.

### Twenty-Node Hexahedral Elements: HEX20_57, HEX20_60, and HEX20_90

Twenty-node hexahedral elements have 60 kinematic degrees of freedom; thus, at least 54 independent forces must be present in their stress interpolation polynomials. Second-order complete polynomials contain 48 independent forces—not enough for the 20-node elements—so cubic polynomials must be used. Complete third-order polynomials were implemented for element HEX20_90, and the stress field developed by Spilker and Singh (ref. 9) was used for element HEX20_57. An additional reduced stress field with 60 independent forces was developed in this study and implemented

for element HEX20_60. It contains 48 independent forces corresponding to complete quadratic polynomials, and 12 additional forces representing cubic terms (given in eqs. (A11)). Both reduced stress fields identically satisfy the equations of equilibrium, and neither element HEX20_57 nor element HEX20_60 possesses zero-energy modes.

For all elements developed here, numerical integration was used to calculate element matrices. For the tetrahedral elements, a 1-point rule that employs the constant stress field was used for element THD04_06; a 5-point rule was used for element THD04_21; and an 11-point rule was used for all other tetrahedral elements. The locations for integration points and the corresponding weights were taken from reference 29. Standard Gauss integration was used for hexahedral elements, with $3 \times 3 \times 3$ points for elements with quadratic stress interpolations, and $4 \times 4 \times 4$ points for elements with cubic stress interpolations.

## Example Problems

A number of example problems are presented in this section in order to demonstrate the accuracy and validity of elements developed in this study. Problems from beam theory, plane stress, and plate bending, for which analytical solutions are available, were selected. Extensive numerical experiments were performed to assess relative performances of the present elements and to compare the Integrated Force Method with the standard displacement method. The responses for one-dimensional problems analyzed here with three-dimensional discretizations are compared to those obtained with two-dimensional models (ref. 23), to verify analogous behavior in corresponding elements.

### Example 1: Bending of a Uniform Cantilever Beam

A cantilever beam of length $L$ with a uniform rectangular cross section of dimensions $d$ by $H$ is shown in figure 2(a). The beam is assumed to be made of a homogeneous and isotropic material with a modulus of elasticity $E$ and a Poisson's ratio $v$; it is subjected to a concentrated force of intensity $P$ at the free end. This beam was analyzed with the entire finite element library in order to verify the present elements and to assess their relative performances. The influence of element shapes on the results was also analyzed. A three-dimensional finite element discretization of the beam is shown in figure 2(b). The support conditions at the clamped end were modeled so as to suppress all three components of the displacement at point $a$ as well as to suppress component $v$ at all nodes in the $xOz$-plane and component $u$ at point $b$. The circles in figure 2(b) denote corner nodes and the asterisks denote midside nodes. Midside nodes are not present in discretizations with four-node tetrahedral elements and eight-
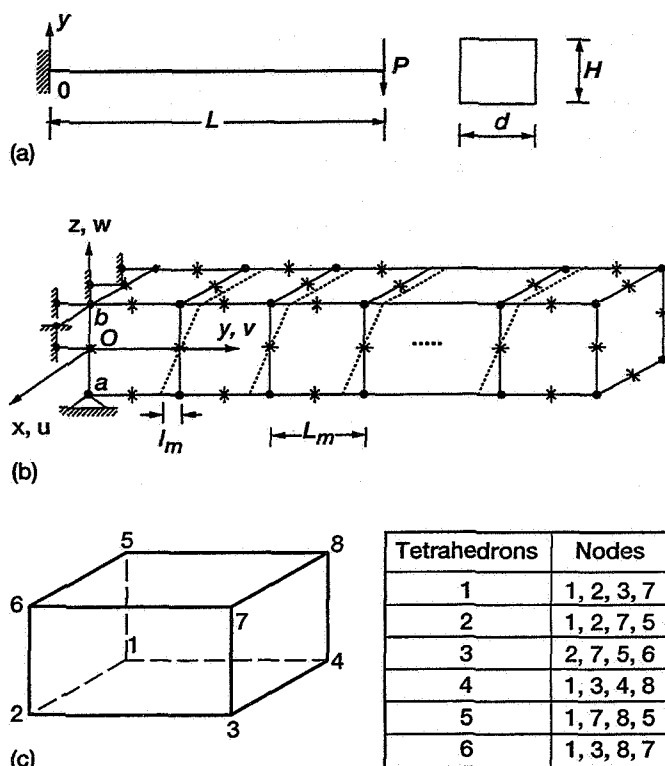
**Figure 2.—Finite element models of a cantilever beam.**
(a) Geometric characteristics and loading of beam.
(b) Finite element discretization. (c) Division of a hexahedral cell into six tetrahedrons.



Figure 3.—Convergence of tip displacement of cantilever beam studied by using tetrahedral elements.

node hexahedral elements. The dashed lines in figure 2(b) denote hexahedral elements of distorted shapes.Discretizations with tetrahedral elements were performed by dividing each hexahedron into six tetrahedrons, as suggested in reference 1. Figure 2(c) shows a typical eight-node hexahedron divided into six four-node tetrahedrons. The table in this figure defines the connectivities of the resulting tetrahedral elements. A hexahedral volume was divided into six 10-node tetrahedrons by introducing additional nodes in the centers of the edges of the original 4-node tetrahedrons.

Let us first consider the displacements of the beam. The convergence of displacement $w$ at the free end was studied. The results are shown in figure 3 for tetrahedral elements, and in figure 4 for hexahedral elements. Also shown in figures 3 and 4 are values obtained by using corresponding isoparametric displacement-based elements. The displacement of the free end was normalized with a closed-form solution $w_{exact}$, which was obtained from one-dimensional beam theory and includes the effect of shear stresses. Figure 3 shows that with 10-node tetrahedral elements, fast convergence is achieved, whereas with 4-node tetrahedral elements, convergence is very slow. Figure 3 also shows that accuracy is not improved by increasing the number of independent forces in stress interpolation polynomials for four-node tetrahedrons.
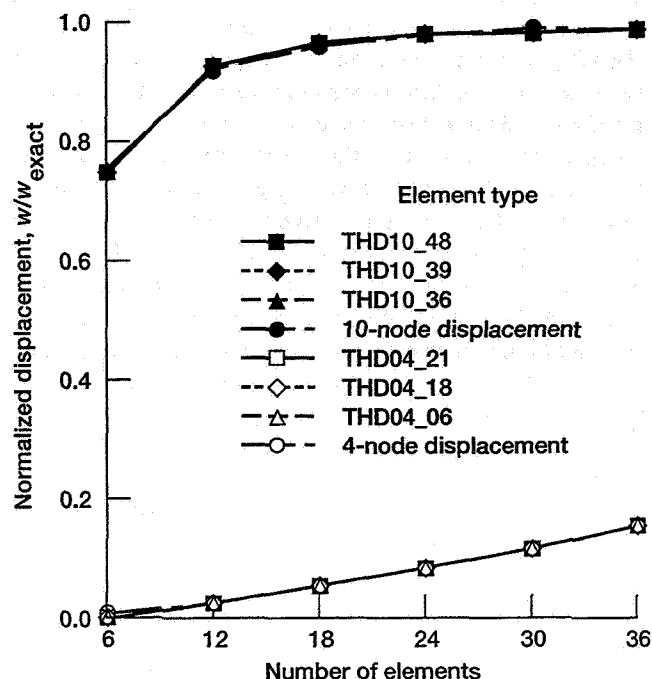
These observations agree with those made in the analysis of a similar problem in which two-dimensional finite element discretizations (ref. 23) using 6-node and 3-node triangles correspond to 10-node and 4-node tetrahedrons, respectively.

The convergence study using hexahedral elements was first performed for elements of rectangular shape. The results of using the present elements, together with those obtained with the standard displacement method, are given in figure 4(a). All 20-node elements from the present library provide very accurate results with a relatively small number of independent forces. A fast convergence is also achieved with element HEX08_18, which employs incomplete second-order polynomials in the stress interpolation matrix. Elements HEX08_48 and HEX08_33, which, respectively, employ complete and reduced quadratic polynomials for the stress interpolation matrix, produce stiff models that lead to slower convergence. A similar behavior was observed in two-dimensional analysis of the beam with a four-node quadrilateral element with bilinear interpolation of the geometry and the displacement fields; in three-dimensional analysis this corresponds to eight-node hexahedral elements. Note that in figure 4(a), the eight-node isoparametric displacement element provides a very slow convergence of displacements, whereas element HEX08_18 achieves very good accuracy with a small number of independent forces. It can, therefore, be concluded that the Integrated Force Method significantly outperforms the standard displacement method in the analyses of certain classes of problems, such as those involving domains of regular shapes.
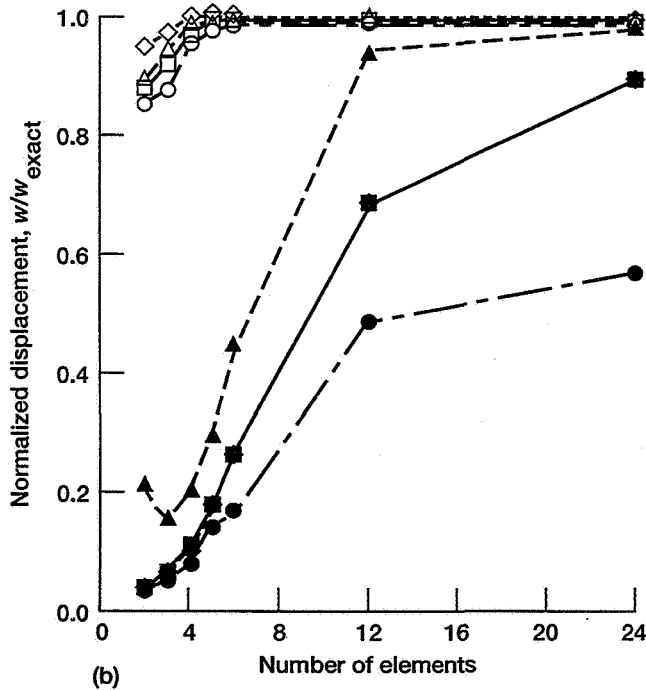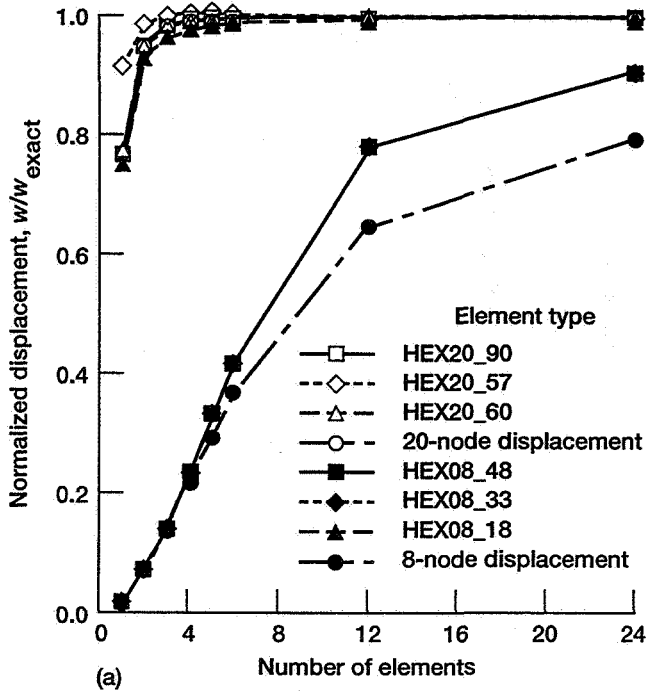
8

Figure 4.—Convergence of tip displacement of cantilever beam studied by using hexahedral elements. (a) Regular meshes. (b) Distorted meshes.

The influence of element shapes on the results was also studied by using distorted meshes to achieve convergence. Distorted elements can be obtained by moving the corner nodes a distance of $l_m = 0.2\,L_m$, as shown in figure 2(b), where $L_m$ is the dimension of the regular-shaped element. The results are shown in figure 4(b). A significant loss of accu-
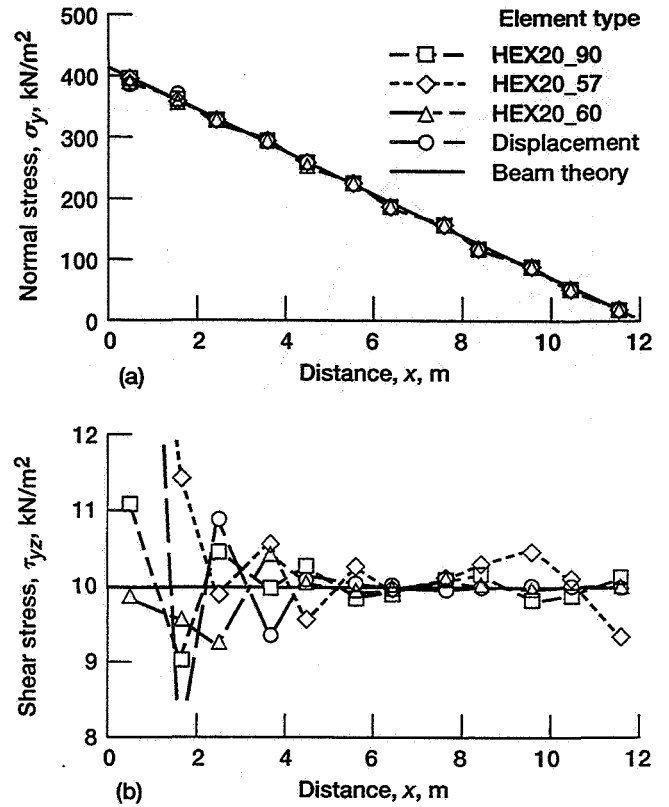


Figure 5.—Stress distribution along line $z = z_g$ of cantilever beam. (a) Normal stress $\sigma_y$. (b) Shear stress $\tau_{yz}$.

racy is suffered by element HEX08_18, whereas the 20-node and 8-node elements with quadratic interpolations of the stress field are little affected. Figure 4(b) also demonstrates that displacement-based isoparametric elements are more sensitive to distortion than corresponding Integrated Force Method elements.

The stresses were calculated next for a beam of length $L = 12.0$ m and cross section $d = H = 1.0$ m; its material properties were assumed to be $E = 21\times10^7$ kN/m$^2$ and $\nu = 0.3$, and the intensity of the concentrated load $P$ was 60 kN. The results obtained with the present elements at normal stress $\sigma_y$ and shear stress $\tau_{yz}$ along the line $z = -z_g = -0.2887$ m are given in figure 5, along with those from the displacement method and the exact solution from the beam theory. Both methods performed well when 20-node elements were used. Note, however, that element HEX08_18 significantly outperformed the corresponding displacement-based element, which exhibited difficulties in stress predictions similar to those observed for the displacements.

### Example 2: Pure Bending of a Circular Arch

A circular arch of radius $r_0$, clamped at $\theta = 0°$ and subjected to a concentrated moment of intensity $M$ at $\theta = 90°$ is shown in figure 6(a). The arch is assumed to have a uniform

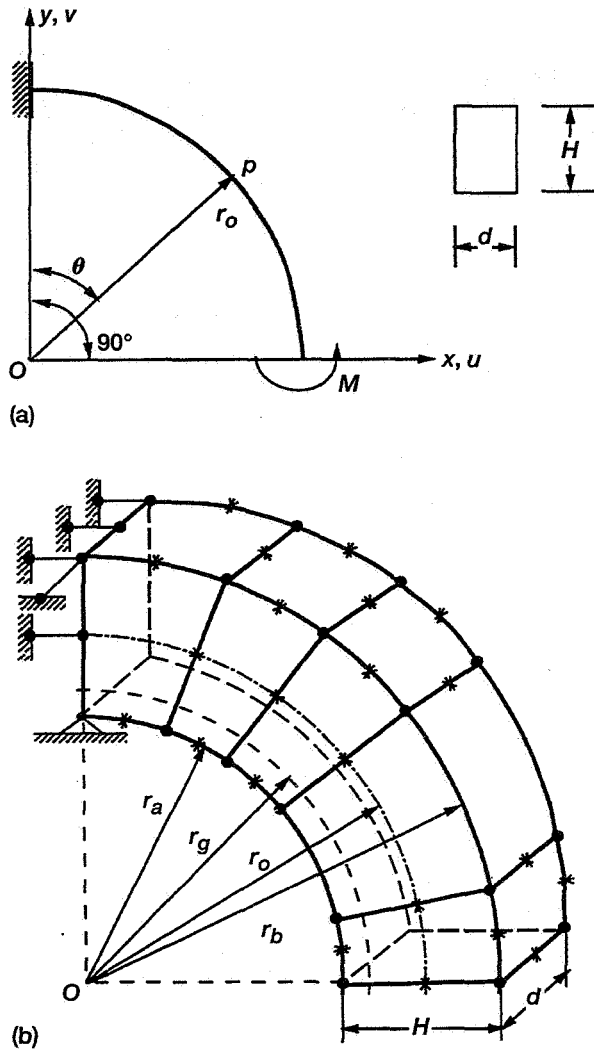Figure 6.—Circular arch subjected to concentrated moment $M$. (a) One-dimensional model. (b) Three-dimensional finite element discretization.



Figure 7.—Convergence of tip displacement $u$ of circular arch.

rectangular cross section of dimensions $d$ by $H$ and to be made of a homogeneous and isotropic material with parameters $E$ and $\nu$. This example is presented to verify the use of the present developments in the analysis of objects with curved contours. A three-dimensional finite element model of the arch is shown in figure 6(b). The asterisks and circles in figure 6(b) represent midside and corner nodes, respectively, as in Example 1. The support conditions for the clamped end were modeled similarly to those of the cantilever beam. The contours of the three-dimensional finite element discretization were defined by cylindrical surfaces with radii $r_a$ and $r_b$, as shown in figure 6(b), where $r_a = r_o - 0.5\,H$, and $r_b = r_o + 0.5\,H$. The arch was analyzed for $r_o = 11.0$ m, $d = 1.0$ m, $H = 2.0$ m, $E = 21 \times 10^7$ N/m$^2$, $\nu = 0.3$, and $M = 600$ kN/m$^2$.

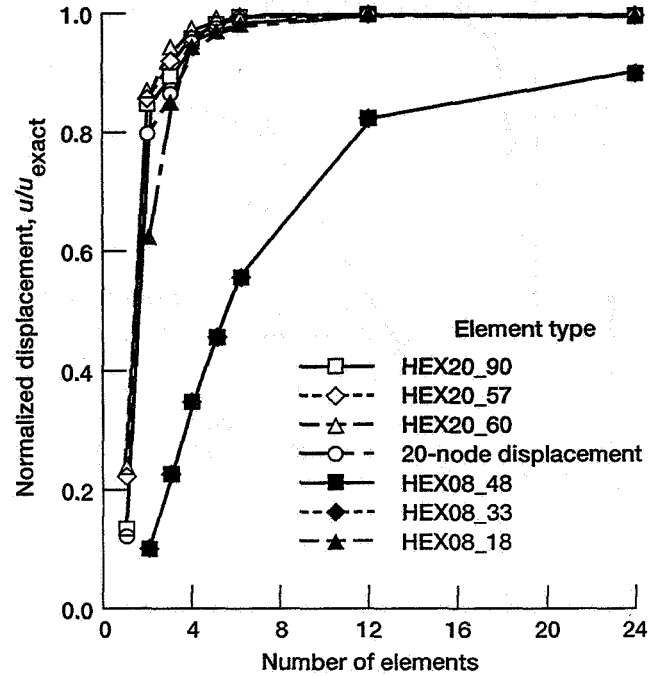First, the convergence of the horizontal displacement component $u$ of the free end was studied. The results obtained by

using present hexahedral elements and those obtained by using a 20-node isoparametric element with the standard displacement method are shown in figure 7. The displacements were normalized with respect to the analytical solution given in reference 30. The present elements performed well, especially the 20-node hexahedrons. The results presented here for element HEX08_18 were obtained by using a local coordinate system with an $Ox$-axis defined by the element centroid $O$ and the centroid of one of the element's sides; an $Oy$-axis normal to the plane defined by the $Ox$-axis and the centroid of the side adjacent to that defining the $Ox$-axis; and an $Oz$-axis orthogonal to the $Oxy$-plane. The results are not shown for the case with the local axes parallel to the global axes, because oscillations were observed in the response and convergence was not achieved. Similar behavior was observed in the two-dimensional analysis of this problem with element QUA04_05, which may be considered to be analogous to element HEX08_18. Both of these elements employ incomplete polynomials with the minimum number of independent forces, and both perform extremely well for domains of rectangular shapes. However, because their stress fields are represented by incomplete polynomials, these elements may become sensitive to the orientation of the coordinate axes. Such behavior demonstrates the benefits of using complete polynomials in stress field representations: the resulting elements are not sensitive to the orientation of local coordinate systems.

Next, the stress distributions for the arch were calculated by using 20-node elements. The results for normal stresses $\sigma_r$ and $\sigma_t$ along the line $r = r_g = 10.423$ m are compared in
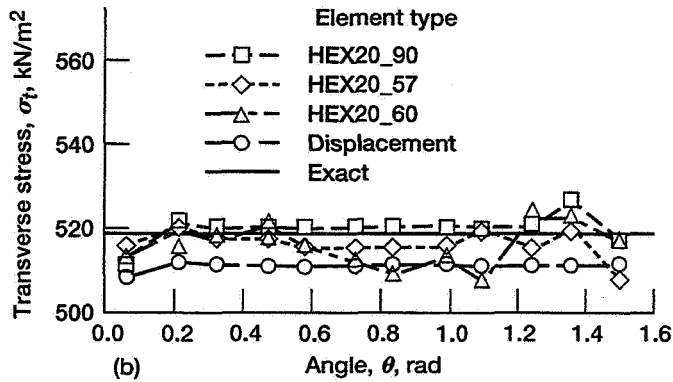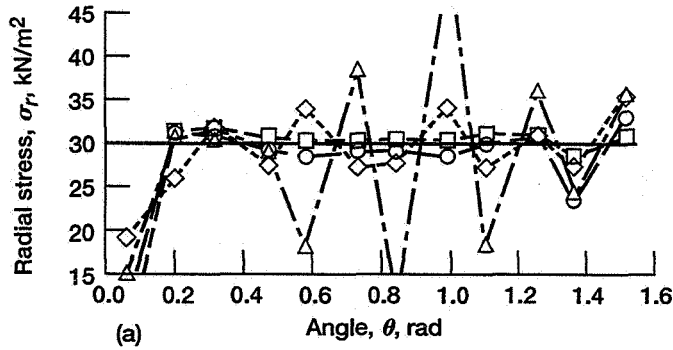
Figure 8.—Stress distribution along line $r = r_g$ of circular arch. (a) Radial stress $\sigma_r$. (b) Transverse stress $\sigma_t$.

figure 8 with the exact values (ref. 30) and with the results from using the 20-node isoparametric element with the displacement method. A good performance of the present elements, especially element HEX20_90, which incorporates complete polynomials, can be seen. There is some loss of accuracy in the results for $\sigma_r$ when elements HEX20_57 and HEX20_60 are used; this is attributed to using reduced polynomials in the stress field approximations. The element HEX20_90, however, provides better stress predictions than the 20-node displacement element.

**Example 3: A Circular Annulus Under Uniform Pressure**

A circular annulus with inner radius $R_i$, outer radius $R_o$, and thickness $d$, subjected to a uniform pressure of intensity $p$ along the inner contour, is depicted in figure 9. The annulus is assumed to be made of a homogeneous and isotropic material with parameters $E$ and $\nu$ and assumed to be in the state of plane stress. Because of the symmetry of the domain and the loading, only a quarter of the annulus was analyzed. A three-dimensional finite element model of the annulus is shown in figure 9(b). The part of the domain analyzed was discretized with two 20-node hexahedral elements in the circumferential direction and $N$ elements in the radial direction. The state of plane stress in the finite element model was achieved by sup-
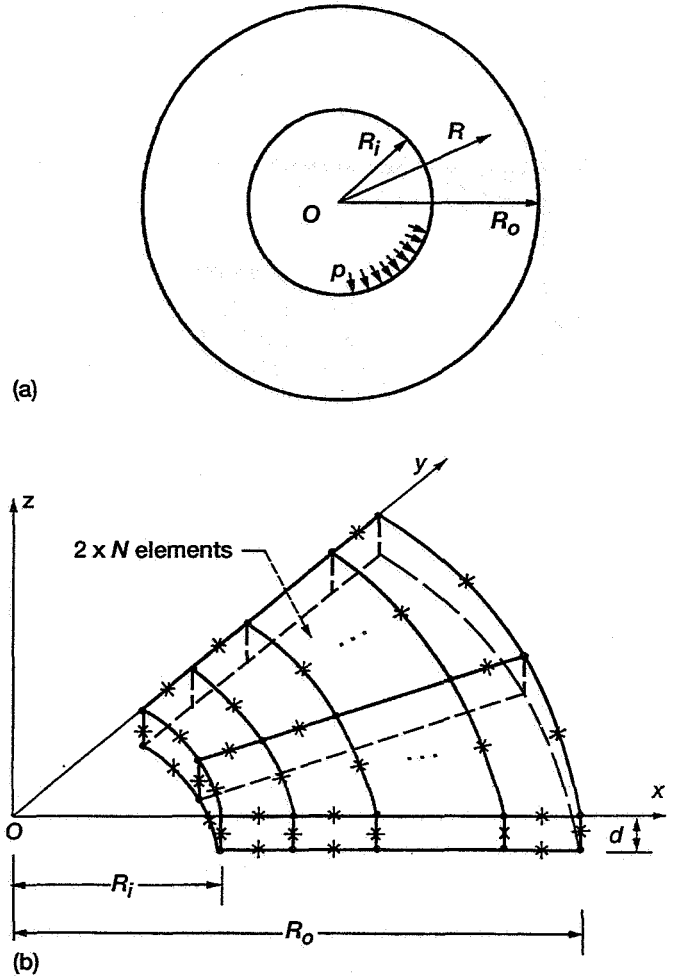


Figure 9.—Annular disk under uniform pressure. (a) Two-dimensional model. (b) Three-dimensional finite element discretization.

pressing the $w$ displacement component of all nodes lying in the plane $z = -0.5\,d$. The symmetry boundary conditions were modeled such that $u = 0$ for nodes in the $x = 0$ plane, and $v = 0$ for nodes in the $y = 0$ plane. Numerical values for the parameters of the annulus were taken as $R_i = 5.0$ m, $R_o = 10.0$ m, $d = 1.0$ m, $E = 21\times10^7$ kN/m$^2$, $\nu = 0.3$, and $p = 10$ kN/m$^2$. A convergence study of the radial displacement $u$ of the inner and the outer surface was performed first. The results obtained with the present elements and those obtained with the 20-node isoparametric displacement method element are shown in figure 10. A fast convergence of the results can be seen.

Stress distributions along the radius of the annulus were obtained next for $N = 5$ elements in the radial direction. The distribution for normal stresses $\sigma_r$ and $\sigma_t$, as determined with the present elements and with the displacement method, are compared in figure 11 with corresponding analytical solutions (ref. 30). Again, there is good agreement of the results. Note that the locations where stresses were calculated correspond
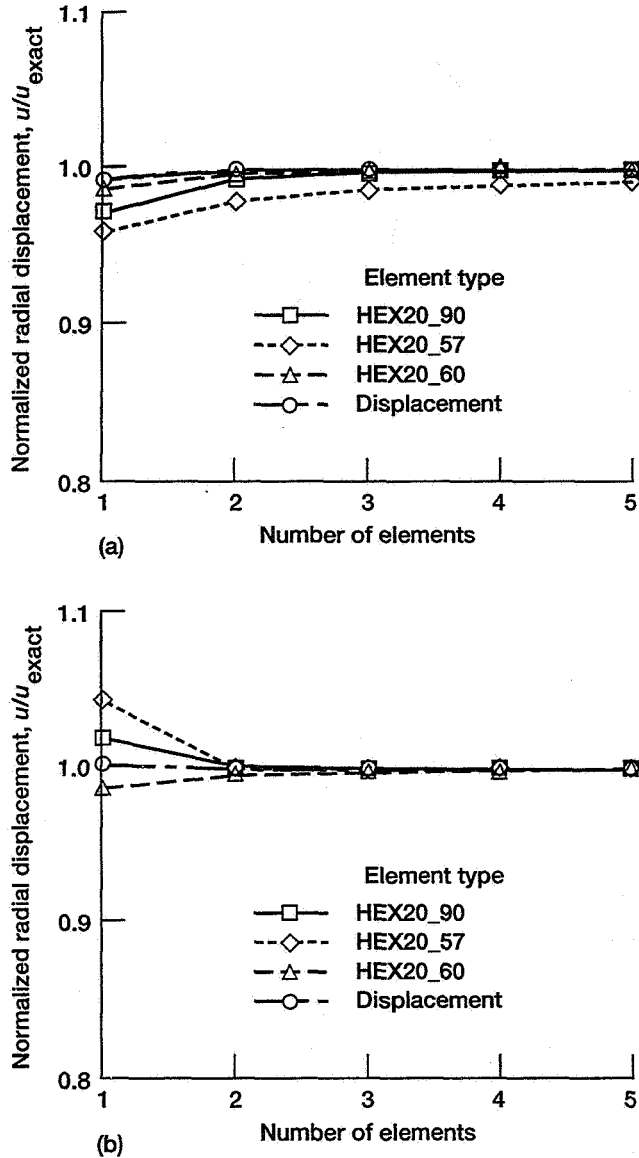
11

Figure 10.—Convergence of annulus radial displacement studied by using hexahedral elements. (a) Inner surface. (b) Outer surface.



Figure 11.—Stress distribution along radius of annulus. (a) Transverse stress $\sigma_t$. (b) Radial stress $\sigma_r$.



Figure 12.—Simply supported rectangular plate in bending.

to Gauss integration points for the $2 \times 2 \times 2$ rule. These points have been shown to be optimal sampling points in the displacement and hybrid methods (ref. 9). The stresses were also calculated at $3 \times 3 \times 3$ Gauss locations, with no loss of accuracy. Thus, it may be concluded that the Integrated Force Method provides a better overall stress response than the displacement method, which generally predicts stress less accurately at locations other than the optimal points.

**Example 4: A Simply Supported Rectangular Plate in Bending**

A rectangular plate of side lengths $2a$ and $2b$ and thickness $h$ is shown in figure 12. The plate is simply supported along
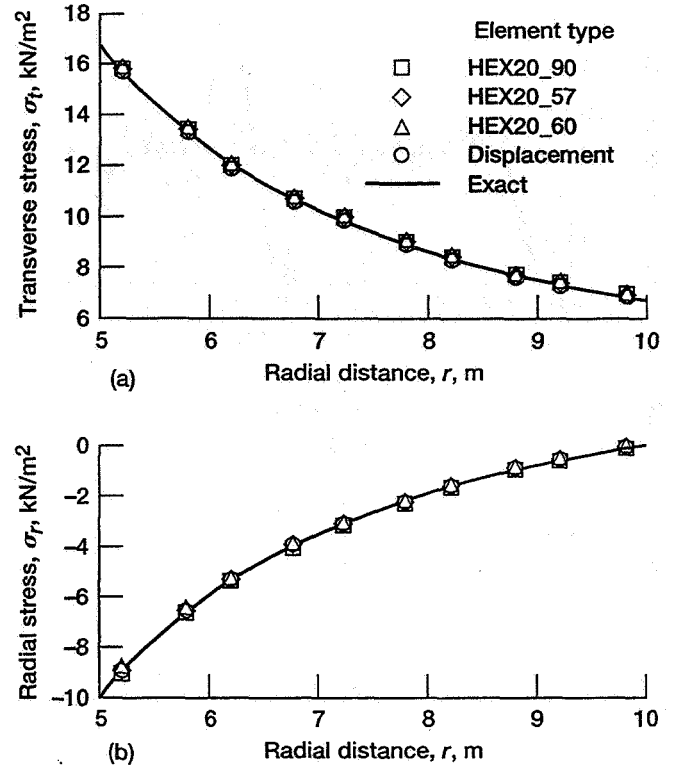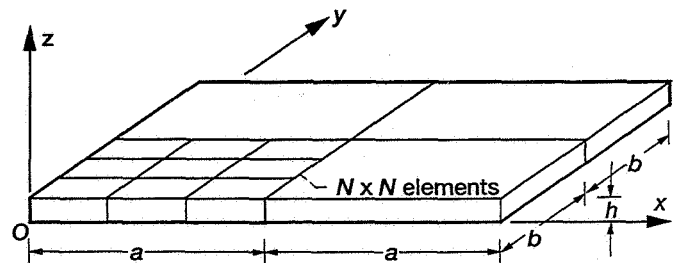
all four sides and is subjected to a uniformly distributed load of intensity $p$ in the direction of the positive $Oz$-axis. The material of the plate is assumed to be homogeneous and isotropic, with parameters $E$ and $v$. Because of the symmetry of its geometric properties and loading, only a quarter of the plate was modeled by using three-dimensional finite elements (see fig. 12). The response of the plate was obtained with both 8-node and 20-node elements. A $4 \times 4$ mesh was used for discretization with the 20-node elements, and a $6 \times 6$ mesh was used for the 8-node elements. Numerical values for geometric and material parameters of the plate and the loading were taken to be $a = b = 20.0$ m, $h = 0.5$ m, $E = 21 \times 10^7$ kN/m$^2$, $v = 0.3$, and $p = 1.0$ kN/m$^2$. The stress distribution for the plate was calculated first. The stresses $\sigma_x$ and $\sigma_{xy}$ along
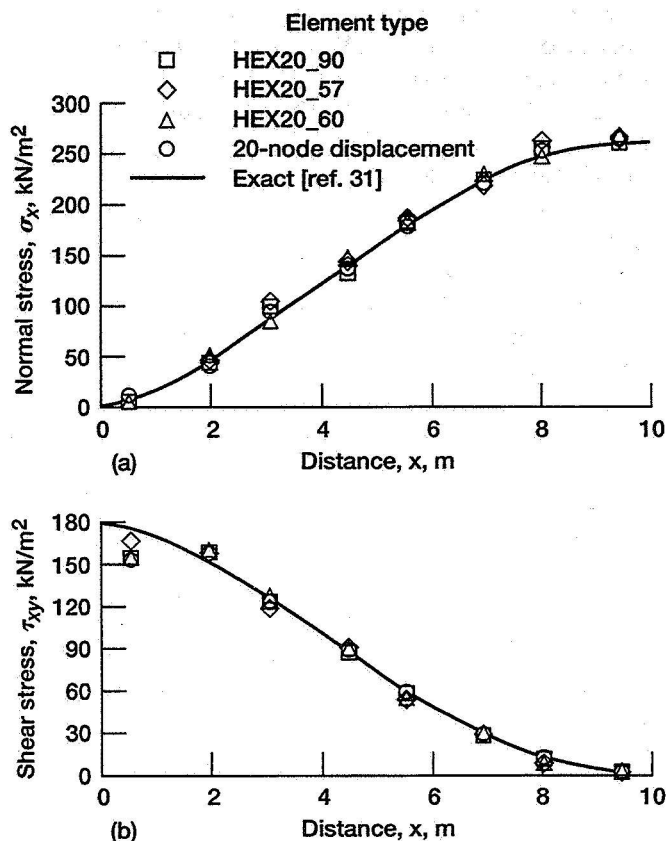
Figure 13.—Stress distribution in plate along line $y = x$.
(a) Normal stress $\sigma_x$. (b) Shear stress $\tau_{xy}$.

the line $y = x$ and for $z = z_g = 0.1057$ m were calculated by using the present elements. They are shown in figure 13 together with the stresses obtained by using the standard displacement method with a 20-node isoparametric element. A comparison with the analytical solution given in reference 31 shows good agreement. The displacements of the plate were calculated next. Lateral displacements for locations along the line $x = a$ were calculated by using both an 8-node and a 20-node element (see fig. 14). All 20-node elements, as well as the element HEX08_18, provided very accurate displacement predictions, but elements HEX08_33 and HEX08_48 produced overly rigid models. The element HEX08_18 again yielded significantly better results than the corresponding eight-node isoparametric displacement element, thereby confirming the conclusions drawn from the results in Example 1.
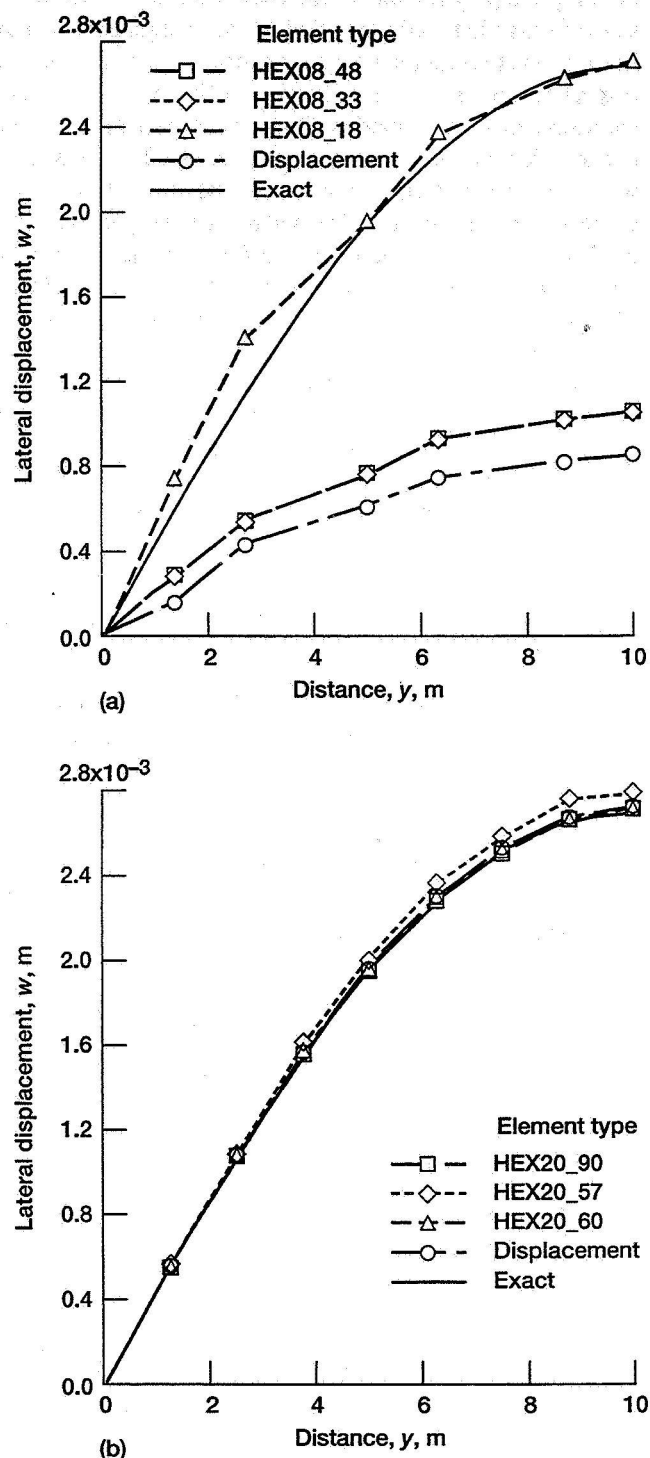


Figure 14.—Displacement distribution in plate along line $x = a$. (a) Eight-node elements. (b) Twenty-node elements.

# Concluding Remarks

The Integrated Force Method was extended in this paper to three-dimensional structural analysis. A general formulation was developed to generate stress field interpolations in terms of complete polynomials of the required order. Such derived stress fields identically satisfied Navier's equations of equilibrium, and the resulting element matrices were invariant with respect to the orientation of local coordinate axes and free of spurious zero-energy modes. The effect of reducing the number of independent forces was also studied. The stress fields were derived in terms of reduced polynomials and then, expressed in terms of complete and reduced polynomials, were used to develop a comprehensive finite element library for three-dimensional structural analysis by the Integrated Force Method. Both tetrahedral- and hexahedral-shaped elements capable of modeling domains with arbitrary configurations were developed. To assess the validity and accuracy of the elements and to compare the Integrated Force Method with the standard displacement method, a number of example problems, whose analytical solutions were known, were solved with the developments presented herein. The following observations can be made on the basis of these numerical experiments:

1. Good accuracy was achieved with all 10-node tetrahedral and 20-node hexahedral elements.

2. The elements that employed the complete polynomials in stress interpolations exhibited the best overall performance and reliability.

3. Although reducing the polynomials used in stress field approximations had no effect on the performance of the corresponding elements in rectangular domains, a certain loss of accuracy was observed in the analysis of domains with curved boundaries.

4. The element HEX08_18 performed extremely well in analyzing rectangular-shaped objects. Applying the element HEX08_18 in the analysis of domains with curved boundaries revealed its sensitivity to the orientation of local coordinate axes.

5. Although good results were obtained with a set of local coordinate systems that followed the curvature of the domain boundaries, unreliable predictions were obtained when the local systems were aligned parallel to the global coordinate system. Thus, element HEX08_18 should be used with caution in the analysis of domains with curved boundaries. Such behavior by element HEX08_18 also justifies the implementation of complete polynomials in stress interpolation matrices.

6. Comparisons of the Integrated Force Method and the standard displacement method revealed good performances by both methods when 10-node tetrahedrons and 20-node hexahedrons were used.

In most cases, the Integrated Force Method performed better overall in stress calculations. However, the eight-node Integrated Force Method elements from the present library demonstrated superior behavior in comparison to the corresponding displacement method element. Thus, for certain classes of problems the Integrated Force Method proved to be the preferred method of analysis. In general, the Integrated Force Method can serve as an alternative to other available formulations.

Lewis Research Center
National Aeronautics and Space Administration
Cleveland, Ohio, June 1, 1995

# Appendix A
## Expressions for Stress Fields

### (a) Complete Polynomials Derived Using the Stress Functions:

– constant terms:

$$\sigma_x^{(o)} = F_1^{(o)} \tag{A1a}$$

$$\sigma_y^{(o)} = F_2^{(o)} \tag{A1b}$$

$$\sigma_z^{(o)} = F_3^{(o)} \tag{A1c}$$

$$\tau_{xy}^{(o)} = F_4^{(o)} \tag{A1d}$$

$$\tau_{yz}^{(o)} = F_5^{(o)} \tag{A1e}$$

$$\tau_{zx}^{(o)} = F_6^{(o)} \tag{A1f}$$

– linear terms:

$$\sigma_x^{(1)} = F_1^{(1)}x + F_2^{(1)}y + F_3^{(1)}z \tag{A2a}$$

$$\sigma_y^{(1)} = F_4^{(1)}x + F_5^{(1)}y + F_6^{(1)}z \tag{A2b}$$

$$\sigma_z^{(1)} = F_7^{(1)}x + F_8^{(1)}y + F_9^{(1)}z \tag{A2c}$$

$$\tau_{xy}^{(1)} = F_{11}^{(1)}x - (F_1^{(1)} + F_{15}^{(1)})y + F_{10}^{(1)}z \tag{A2d}$$

$$\tau_{yz}^{(1)} = F_{12}^{(1)}x + F_{13}^{(1)}y - (F_5^{(1)} + F_{11}^{(1)})z \tag{A2e}$$

$$\tau_{zx}^{(1)} = -(F_9^{(1)} + F_{13}^{(1)})x + F_{14}^{(1)}y + F_{15}^{(1)}z \tag{A2f}$$

– quadratic terms:

$$\sigma_x^{(2)} = F_1^{(2)}x^2 + F_2^{(2)}y^2 + F_3^{(2)}z^2 + F_4^{(2)}xy + F_5^{(2)}yz + F_6^{(2)}zx \tag{A3a}$$

$$\sigma_y^{(2)} = F_7^{(2)}x^2 + F_8^{(2)}y^2 + F_9^{(2)}z^2 + F_{10}^{(2)}xy + F_{11}^{(2)}yz + F_{12}^{(2)}zx \tag{A3b}$$

$$\sigma_z^{(2)} = F_{13}^{(2)}x^2 + F_{14}^{(2)}y^2 + F_{15}^{(2)}z^2 + F_{16}^{(2)}xy + F_{17}^{(2)}yz + F_{18}^{(2)}zx \tag{A3c}$$

$$\tau_{xy}^{(2)} = F_{19}^{(2)}x^2 + F_{20}^{(2)}y^2 + F_{21}^{(2)}z^2 - (F_1^{(2)} + F_8^{(2)} - F_{15}^{(2)})xy - (F_6^{(2)} + 2F_{27}^{(2)})yz$$
$$- (F_{11}^{(2)} + 2F_{24}^{(2)})zx \tag{A3d}$$

$$\tau_{yz}^{(2)} = F_{22}^{(2)}x^2 + F_{23}^{(2)}y^2 + F_{24}^{(2)}z^2 - (F_{18}^{(2)} + 2F_{25}^{(2)})xy + (F_1^{(2)} - F_8^{(2)} - F_{15}^{(2)})yz$$
$$- (F_{10}^{(2)} + 2F_{19}^{(2)})zx \tag{A3e}$$

$$\tau_{zx}^{(2)} = F_{25}^{(2)}x^2 + F_{26}^{(2)}y^2 + F_{27}^{(2)}z^2 - (F_{17}^{(2)} + 2F_{23}^{(2)})xy - (F_4^{(2)} + 2F_{20}^{(2)})yz$$
$$- (F_1^{(2)} - F_8^{(2)} + F_{15}^{(2)})yz \tag{A3f}$$

– cubic terms:

$$\sigma_x^{(3)} = F_1^{(3)}x^3 + F_2^{(3)}y^3 + F_3^{(3)}z^3 + F_4^{(3)}x^2y + F_5^{(3)}xy^2$$
$$+ F_6^{(3)}y^2z + F_7^{(3)}yz^2 + F_8^{(3)}z^2x + F_9^{(3)}zx^2 - 2(F_{31}^{(3)} + F_{42}^{(3)})xyz \tag{A4a}$$

$$\sigma_y^{(3)} = F_{10}^{(3)} x^3 + F_{11}^{(3)} y^3 + F_{12}^{(3)} z^3 + F_{13}^{(3)} x^2 y + F_{14}^{(3)} xy^2$$
$$+ \ F_{15}^{(3)} y^2 z + F_{16}^{(3)} yz^2 + F_{17}^{(3)} z^2 x + F_{18}^{(3)} zx^2 - 2(F_{32}^{(3)} + F_{37}^{(3)}) xyz \tag{A4b}$$

$$\sigma_z^{(3)} = F_{19}^{(3)} x^3 + F_{20}^{(3)} y^3 + F_{21}^{(3)} z^3 + F_{22}^{(3)} x^2 y + F_{23}^{(3)} xy^2$$
$$+ \ F_{24}^{(3)} y^2 z + F_{25}^{(3)} yz^2 + F_{26}^{(3)} z^2 x + F_{27}^{(3)} zx^2 - 2(F_{36}^{(3)} + F_{41}^{(3)}) xyz \tag{A4c}$$

$$\tau_{xy}^{(3)} = F_{28}^{(3)} x^3 + F_{29}^{(3)} y^3 + F_{30}^{(3)} z^3 + \frac{1}{2}(F_{26}^{(3)} - 3F_1^{(3)} - F_{14}^{(3)}) x^2 y$$
$$+ \ \frac{1}{2}(F_{25}^{(3)} - 3F_{11}^{(3)} - F_4^{(3)}) xy^2 + F_{31}^{(3)} y^2 z - (F_8^{(3)} + 3F_{40}^{(3)}) yz^2 - (F_{16}^{(3)} + 3F_{35}^{(3)}) z^2 x$$
$$+ \ F_{32}^{(3)} zx^2 + (3F_{21}^{(3)} - F_9^{(3)} - F_{15}^{(3)}) xyz \tag{A4d}$$

$$\tau_{yz}^{(3)} = F_{33}^{(3)} x^3 + F_{34}^{(3)} y^3 + F_{35}^{(3)} z^3 - (F_{27}^{(3)} + 3F_{38}^{(3)}) x^2 y + F_{36}^{(3)} xy^2$$
$$+ \ \frac{1}{2}(F_4^{(3)} - 3F_{11}^{(3)} - F_{25}^{(3)}) y^2 z - \frac{1}{2}(F_9^{(3)} - 3F_{21}^{(3)} - F_{15}^{(3)}) yz^2 + F_{37}^{(3)} z^2 x$$
$$- \ (F_{13}^{(3)} + 3F_{28}^{(3)}) zx^2 + (3F_1^{(3)} - F_{14}^{(3)} - F_{26}^{(3)}) xyz \tag{A4e}$$

$$\tau_{zx}^{(3)} = F_{38}^{(3)} x^3 + F_{39}^{(3)} y^3 + F_{40}^{(3)} z^3 + F_{41}^{(3)} x^2 y - (F_{24}^{(3)} + 3F_{34}^{(3)}) xy^2$$
$$- \ (F_5^{(3)} + 3F_{29}^{(3)}) y^2 z - F_{42}^{(3)} yz^2 + \frac{1}{2}(F_{15}^{(3)} - 3F_{21}^{(3)} - F_9^{(3)}) z^2 x +$$
$$+ \ \frac{1}{2}(F_{14}^{(3)} - 3F_1^{(3)} - F_{26}^{(3)}) zx^2 + (3F_{11}^{(3)} - F_4^{(3)} - F_{25}^{(3)}) xyz \tag{A4f}$$

The superscripts 0, 1, 2, and 3 in Eqs.(A1) - (A4) denote the stress components and the independent forces that correspond to constant, linear, quadratic and cubic terms in the stress interpolations, respectively.

– complete cubic polynomial:

$$\sigma_x = F_1 + F_7 x + F_8 y + F_9 z + F_{22} x^2 + F_{23} y^2 + F_{24} z^2 + F_{25} xy + F_{26} yz + F_{27} zx$$
$$+ \ F_{49} x^3 + F_{50} y^3 + F_{51} z^3 + F_{52} x^2 y + F_{53} xy^2 + F_{54} y^2 z + F_{55} yz^2 + F_{56} z^2 x + F_{57} zx^2$$
$$- \ 2(F_{79} + F_{90}) xyz \tag{A5a}$$

$$\sigma_y = F_2 + F_{10} x + F_{11} y + F_{12} z + F_{28} x^2 + F_{29} y^2 + F_{30} z^2 + F_{31} xy + F_{32} yz + F_{33} zx$$
$$+ \ F_{58} x^3 + F_{59} y^3 + F_{60} z^3 + F_{61} x^2 y + F_{62} xy^2 + F_{63} y^2 z + F_{64} yz^2 + F_{65} z^2 x + F_{66} zx^2$$
$$- \ 2(F_{80} + F_{85}) xyz \tag{A5b}$$

$$\sigma_z = F_3 + F_{13} x + F_{14} y + F_{15} z + F_{34} x^2 + F_{35} y^2 + F_{36} z^2 + F_{37} xy + F_{38} yz + F_{39} zx$$
$$+ \ F_{67} x^3 + F_{68} y^3 + F_{69} z^3 + F_{70} x^2 y + F_{71} xy^2 + F_{72} y^2 z + F_{73} yz^2 + F_{74} z^2 x + F_{75} zx^2$$
$$- \ 2(F_{84} + F_{89}) xyz \tag{A5c}$$

$$\tau_{xy} = F_4 + F_{17} x - (F_7 + F_{21}) y + F_{16} z + F_{40} x^2 + F_{41} y^2 + F_{42} z^2$$
$$- \ (F_{22} + F_{29} - F_{36}) xy - (F_{27} + 2F_{48}) yz - (F_{32} + 2F_{45}) zx$$
$$+ \ F_{76} x^3 + F_{77} y^3 + F_{78} z^3 + \frac{1}{2}(F_{74} - 3F_{49} - F_{62}) x^2 y + \frac{1}{2}(F_{73} - 3F_{59} - F_{52}) xy^2$$
$$+ \ F_{79} y^2 z - (F_{56} + 3F_{88}) yz^2 - (F_{64} + 3F_{83}) z^2 x + F_{80} zx^2$$
$$+ \ (3F_{69} - F_{57} - F_{63}) xyz \tag{A5d}$$

16

$$\tau_{yz} = F_5 + F_{18}x + F_{19}y - (F_{11} + F_{17})z + F_{43}x^2 + F_{44}y^2 + F_{45}z^2$$
$$- (F_{39} + 2F_{46})xy + (F_{22} - F_{29} - F_{36})yz - (F_{31} + 2F_{40})zx$$
$$+ F_{81}x^3 + F_{82}y^3 + F_{83}z^3 - (F_{75} + 3F_{86})x^2y + F_{84}xy^2 + \frac{1}{2}(F_{52} - 3F_{59} - F_{73})y^2z$$
$$- \frac{1}{2}(F_{57} - 3F_{69} - F_{63})yz^2 + F_{85}z^2x - (F_{61} + 3F_{76})zx^2$$
$$+ (3F_{49} - F_{62} - F_{74})xyz \tag{A5e}$$

$$\tau_{zx} = F_6 - (F_{15} + F_{19})x + F_{20}y + F_{21}z + F_{46}x^2 + F_{47}y^2 + F_{48}z^2$$
$$- (F_{38} + 2F_{44})xy - (F_{25} + 2F_{41})yz - (F_{22} - F_{29} + F_{36})zx$$
$$+ F_{86}x^3 + F_{87}y^3 + F_{88}z^3 + F_{89}x^2y - (F_{72} + 3F_{82})xy^2 - (F_{53} + 3F_{77})y^2z + F_{90}yz^2$$
$$+ \frac{1}{2}(F_{63} - 3F_{69} - F_{57})z^2x + \frac{1}{2}(F_{62} - 3F_{49} - F_{74})zx^2$$
$$+ (3F_{59} - F_{52} - F_{73})xyz \tag{A5f}$$

**(b) Robinson's Stress Field [5]:**

$$\sigma_x = F_1 + F_2y + F_3z + F_4yz \tag{A6a}$$
$$\sigma_y = F_5 + F_6z + F_7x + F_8zx \tag{A6b}$$
$$\sigma_z = F_9 + F_{10}x + F_{11}y + F_{12}xy \tag{A6c}$$
$$\tau_{xy} = F_{13} + F_{14}z \tag{A6d}$$
$$\tau_{yz} = F_{15} + F_{16}x \tag{A6e}$$
$$\tau_{zx} = F_{17} + F_{18}y \tag{A6f}$$

**(c) Spilker's Stress Field [9]:**

$$\sigma_x = F_1 - (F_{13} + F_{24} + 2F_{36} + 2F_{51})x + F_2y + F_3z$$
$$- (F_7 + F_8 + F_{18} + F_{29})x^2 + 2F_7y^2 + 2F_8z^2$$
$$+ (F_4 - F_{15} - F_{26} - 2F_{41})xy + F_5yz + (F_6 - F_{17} - F_{28} - F_{39})zx$$
$$+ \frac{1}{3}(2F_{22} + 2F_{33} + F_{54} + F_{56})x^3$$
$$- \frac{1}{3}(F_{10} + F_{11} + F_{21} - F_{22} + F_{32} - F_{33} + F_{52} + F_{53} - F_{54} + F_{55} - F_{56} + F_{57})(y^3 + z^3)$$
$$+ F_{52}x^2y - F_{33}xy^2 + F_{10}y^2z + F_{11}yz^2 - F_{22}z^2x + F_{53}zx^2 + (F_9 - F_{20} - F_{31})xyz \tag{A7a}$$

$$\sigma_y = F_{12} + F_{13}x - (F_2 + F_{25} + 2F_{35} + 2F_{46})y + F_{14}z$$
$$+ 2F_{18}x^2 - (F_7 + F_{18} + F_{19} + F_{30})y^2 + 2F_{19}z^2$$
$$- (F_4 - F_{15} + F_{26} + 2F_{40})xy - (F_5 - F_{16} + F_{27} + 2F_{42})yz + F_{17}zx$$
$$+ \frac{1}{3}(2F_{11} + 2F_{32} + F_{52} + F_{57})y^3$$
$$- \frac{1}{3}(F_{10} - F_{11} + F_{21} + F_{22} - F_{32} + F_{33} - F_{52} + F_{53} + F_{54} + F_{55} + F_{56} - F_{57})(z^3 + x^3)$$
$$- F_{32}x^2y + F_{54}xy^2 + F_{55}y^2z - F_{11}yz^2 + F_{22}z^2x + F_{21}zx^2$$

17

$$- \ (F_9 - F_{20} + F_{31})xyz \tag{A7b}$$

$$\begin{aligned}
\sigma_z \ = \ & F_{23} + F_{24}x + F_{25}y - (F_3 + F_{14} + 2F_{45} + 2F_{50})z \\
+ \ & 2F_{29}x^2 + 2F_{30}y^2 - (F_8 + F_{19} + F_{29} + F_{30})z^2 \\
+ \ & F_{26}xy - (F_5 + F_{16} - F_{27} + 2F_{48})yz - (F_6 + F_{17} - F_{28} + 2F_{47})zx \\
+ \ & \frac{1}{3}(2F_{10} + 2F_{21} + F_{53} + F_{55})z^3 \\
+ \ & \frac{1}{3}(F_{10} - F_{11} + F_{21} - F_{22} - F_{32} - F_{33} - F_{52} + F_{53} - F_{54} + F_{55} - F_{56} - F_{57})(x^3 + y^3) \\
+ \ & F_{32}x^2y + F_{33}xy^2 - F_{10}y^2z + F_{57}yz^2 + F_{56}z^2x - F_{21}zx^2 \\
- \ & (F_9 + F_{20} - F_{31})xyz \tag{A7c}
\end{aligned}$$

$$\begin{aligned}
\tau_{xy} \ = \ & F_{34} + (F_2 + 2F_{35})x + (F_{13} + 2F_{36})y + (F_{37} + F_{38})z \\
+ \ & \frac{1}{2}(F_4 - \frac{1}{2}F_{15})x^2 - \frac{1}{2}(\frac{1}{2}F_4 - F_{15})y^2 + (F_{40} + F_{41})z^2 \\
+ \ & 2(F_7 + F_{18})xy - (\frac{1}{2}F_6 - F_{17} - 2F_{39})yz + (F_5 - \frac{1}{2}F_{16} + 2F_{42})zx \\
- \ & \frac{2}{3}(F_{10} + F_{21} + F_{53} + F_{55})z^3 - (F_{22} + F_{33} + F_{54})x^2y - (F_{11} + F_{32} + F_{52})xy^2 \\
- \ & \frac{1}{2}(\frac{1}{2}F_9 - F_{20})y^2z + F_{22}yz^2 + F_{11}z^2x + \frac{1}{2}(F_9 - \frac{1}{2}F_{20})x^2z \\
+ \ & 2(F_{10} + F_{21})xyz \tag{A7d}
\end{aligned}$$

$$\begin{aligned}
\tau_{yz} \ = \ & F_{43} + (F_{38} + F_{44})x + (F_{14} + 2F_{45})y + (F_{25} + 2F_{46})z \\
+ \ & (F_{42} + F_{48})x^2 + \frac{1}{2}(F_{16} - \frac{1}{2}F_{27})y^2 - \frac{1}{2}(\frac{1}{2}F_{16} - F_{27})z^2 \\
+ \ & (F_{17} - \frac{1}{2}F_{28} + 2F_{47})xy + 2(F_{19} + F_{30})yz - (\frac{1}{2}F_{15} - F_{26} - 2F_{40})zx \\
- \ & \frac{2}{3}(F_{22} + F_{33} + F_{54} + F_{56})x^3 + F_{21}x^2y + \frac{1}{2}(F_{20} - \frac{1}{2}F_{31})xy^2 + (F_{10} + F_{21} - F_{55})yz^2 \\
- \ & (F_{11} + F_{32} + F_{57})y^2z - \frac{1}{2}(\frac{1}{2}F_{20} - F_{31})z^2x + F_{32}zx^2 \\
+ \ & 2(F_{22} + F_{33})xyz \tag{A7e}
\end{aligned}$$

$$\begin{aligned}
\tau_{zx} \ = \ & F_{49} + (F_3 + 2F_{50})x + (F_{37} + F_{44})y + (F_{24} + 2F_{51})z \\
+ \ & \frac{1}{2}(F_6 - \frac{1}{2}F_{28})x^2 + (F_{39} + F_{47})y^2 - \frac{1}{2}(\frac{1}{2}F_6 - F_{28})z^2 \\
+ \ & (F_5 - \frac{1}{2}F_{27} + 2F_{48})xy - (\frac{1}{2}F_4 - F_{26} - 2F_{41})yz + 2(F_8 + F_{29})zx \\
- \ & \frac{2}{3}(F_{11} + F_{32} + F_{52} + F_{57})y^3 + \frac{1}{2}(F_9 - \frac{1}{2}F_{31})x^2y + F_{10}xy^2 \\
+ \ & F_{33}y^2z - \frac{1}{2}(\frac{1}{2}F_9 - F_{31})yz^2 - (F_{22} + F_{33} + F_{56})x^2z - (F_{10} + F_{21} + F_{53})xz^2 \\
+ \ & 2(F_{11} + F_{32})xyz \tag{A7f}
\end{aligned}$$

**(e) Quadratic Terms for the Stress Field in the Element HEX08_33:**

$$\sigma_x^{(2r)} \ = \ F_1^{(2r)}y^2 + F_2^{(2r)}z^2 + F_3^{(2r)}yz \tag{A8a}$$

$$\sigma_y^{(2r)} \ = \ F_4^{(2r)}z^2 + F_5^{(2r)}x^2 + F_6^{(2r)}zx \tag{A8b}$$

$$\sigma_z^{(2r)} = F_7^{(2r)}x^2 + F_8^{(2r)}y^2 + F_9^{(2r)}xy \tag{A8c}$$

$$\tau_{xy}^{(2r)} = F_{10}^{(2r)}z^2 \tag{A8d}$$

$$\tau_{yz}^{(2r)} = F_{11}^{(2r)}x^2 \tag{A8e}$$

$$\tau_{zx}^{(2r)} = F_{12}^{(2r)}y^2 \tag{A8f}$$

**(f) Quadratic Terms for the Stress Field in the Element THD10_39:**

$$\sigma_x^{(2r)} = F_1^{(2r)}x^2 + F_2^{(2r)}y^2 + F_3^{(2r)}z^2 + F_4^{(2r)}xy + F_5^{(2r)}yz + F_6^{(2r)}zx \tag{A9a}$$

$$\sigma_y^{(2r)} = F_7^{(2r)}x^2 + F_8^{(2r)}y^2 + F_9^{(2r)}z^2 + F_{10}^{(2r)}xy + F_{11}^{(2r)}yz + F_{12}^{(2r)}zx \tag{A9b}$$

$$\sigma_z^{(2r)} = F_{13}^{(2r)}x^2 + F_{14}^{(2r)}y^2 + F_{15}^{(2r)}z^2 + F_{16}^{(2r)}xy + F_{17}^{(2r)}yz + F_{18}^{(2r)}zx \tag{A9c}$$

$$\tau_{xy}^{(2r)} = (-F_1^{(2r)} - F_8^{(2r)} + F_{15}^{(2r)})xy - F_6^{(2r)}yz - F_{11}^{(2r)}zx \tag{A9d}$$

$$\tau_{yz}^{(2r)} = -F_{18}^{(2r)}xy + (F_1^{(2r)} - F_8^{(2r)} - F_{15}^{(2r)})yz - F_{10}^{(2r)}zx \tag{A9e}$$

$$\tau_{zx}^{(2r)} = -F_{17}^{(2r)}xy - F_4^{(2r)}yz - (F_1^{(2r)} - F_8^{(2r)} + F_{15}^{(2r)})zx \tag{A9f}$$

**(f) Quadratic Terms for the Stress Field in the Element TET10_36:**

$$\sigma_x^{(2r)} = F_1^{(2r)}xy + F_2^{(2r)}yz + F_3^{(2r)}zx + F_{10}^{(2r)}x^2 + F_{13}^{(2r)}(y^2 + z^2) \tag{A10a}$$

$$\sigma_y^{(2r)} = F_4^{(2r)}xy + F_5^{(2r)}yz + F_6^{(2r)}zx + F_{11}^{(2r)}y^2 + F_{14}^{(2r)}(z^2 + x^2) \tag{A10b}$$

$$\sigma_z^{(2r)} = F_7^{(2r)}xy + F_8^{(2r)}yz + F_9^{(2r)}zx + F_{12}^{(2r)}z^2 + F_{15}^{(2r)}(x^2 + y^2) \tag{A10c}$$

$$\tau_{xy}^{(2r)} = (-F_{10}^{(2r)} - F_{11}^{(2r)} + F_{12}^{(2r)})xy - F_3^{(2r)}yz - F_5^{(2r)}zx \tag{A10d}$$

$$\tau_{yz}^{(2r)} = -F_9^{(2r)}xy + (F_{10}^{(2r)} - F_{11}^{(2r)} - F_{12}^{(2r)})yz - F_4^{(2r)}zx \tag{A10e}$$

$$\tau_{zx}^{(2r)} = -F_8^{(2r)}xy - F_1^{(2r)}yz + (F_{10}^{(2r)} - F_{11}^{(2r)} + F_{12}^{(2r)})zx \tag{A10f}$$

**(h) Cubic Terms for the Stress Field in the Element HEX20_60:**

$$\sigma_x^{(3r)} = F_1^{(3r)}yz^2 + F_2^{(3r)}y^2z + F_8^{(3r)}x^3 + F_7^{(3r)}xyz + 3F_{12}^{(3r)}x^2z \tag{A11a}$$

$$\sigma_y^{(3r)} = F_3^{(3r)}z^2x + F_4^{(3r)}zx^2 + F_{10}^{(3r)}y^3 + F_9^{(3r)}xyz + 3F_8^{(3r)}xy^2 \tag{A11b}$$

$$\sigma_z^{(3r)} = F_5^{(3r)}xy^2 + F_6^{(3r)}x^2y + F_{12}^{(3r)}z^3 + F_{11}^{(3r)}xyz + 3F_{10}^{(3r)}yz^2 \tag{A11c}$$

$$\tau_{xy}^{(3r)} = -3F_8x^2y - \frac{1}{2}F_7y^2z \tag{A11d}$$

$$\tau_{yz}^{(3r)} = -3F_{10}y^2z - \frac{1}{2}F_9xz^2 \tag{A11e}$$

$$\tau_{zx}^{(3r)} = -3F_{12}z^2x - \frac{1}{2}F_{11}xy^2 \tag{A11f}$$

19

# Appendix B
## Symbols

| | | | |
|---|---|---|---|
| $\{\mathbf{B}_e\}$ | element equilibrium matrix; $\int_V (\mathbf{Z})^{\mathsf{T}}[\mathbf{Y}]\mathrm{d}V$ | $N_s$ | number of prescribed displacements |
| $[\mathbf{B}_p]$ | portion of system equilibrium matrix corresponding to nodes where external loads are prescribed | $N_t$ | total number of displacement degrees of freedom |
| $[\mathbf{B}_s]$ | portion of system equilibrium matrix corresponding to nodes with prescribed displacement boundary conditions | $n$ | number of system equilibrium equations; $N_t - N_s$ |
| $[\mathbf{C}]$ | compatibility matrix | $O\bar{x}, O\bar{y}, O\bar{z}$ | global coordinate axes |
| $C_{i,j}^k$ | arbitrary coefficients | $\{\mathbf{P}\}$ | vector of system equivalent nodal loads |
| $[\mathbf{D}]$ | compliance matrix of material | $\{\mathbf{P}_e\}$ | vector of element equivalent nodal loads |
| $d$ | cross sectional dimension | $[\mathbf{P}^*]$ | $\{\mathbf{P}^*\} = \left\{ \begin{matrix} \{\mathbf{P}\} \\ \{\mathbf{0}\} \end{matrix} \right\}$ |
| $E$ | modulus of elasticity | $p$ | order of polynomial |
| $\{\mathbf{F}\}$ | system vector of independent forces | $Q$ | number of independent generalized forces |
| $\{\mathbf{F}_e\}$ | vector of element independent generalized forces | $\{\mathbf{R}\}$ | vector of support reactions; $\{\mathbf{B}_s\}\{\mathbf{F}\}$ |
| $\mathbf{F}_i$ | generalized force coefficients | $R_i, R_o$ | inner, outer radius of circular annulus |
| $[\mathbf{G}]$ | system flexibility matrix | $r$ | number of compatibility conditions |
| $\{\mathbf{G}_e\}$ | element flexibility matrix; $\int_V (\mathbf{Y})^{\mathsf{T}}[\mathbf{D}][\mathbf{Y}]\mathrm{d}V$ | $r,\theta$ | polar coordinates |
| $H$ | cross sectional dimension | $r_a$ | radius to inside of arch |
| $[\mathbf{J}]$ | $n \times m$ deformation matrix; represents top $n$ rows of $[\mathbf{S}]^{-1}$ | $r_b$ | radius to outside of arch |
| | | $r_g$ | radius of Gauss point |
| $[\mathbf{L}]$ | matrix of differential operators that defines strain-displacement relationship | $r_o$ | radius of circular arch |
| $L$ | length | $[\mathbf{S}]$ | $[\mathbf{S}] = \begin{bmatrix} [\mathbf{B}_p] \\ [\mathbf{C}][\mathbf{G}] \end{bmatrix}$ |
| $l_m$ | distance corner node is moved | $\{\mathbf{U}\}$ | vector of unknown nodal displacements; $[\mathbf{J}][\mathbf{G}]\{\mathbf{F}\}$ |
| $M$ | intensity of moment | | |
| $m$ | number of independent forces | $\{\mathbf{U}_e\}$ | vector of displacement at element nodes resulting from finite element discretization |
| $[\mathbf{N}]$ | matrix of displacement interpolation functions | $\{\mathbf{u}\}$ | displacement vector |

20

| | | | | |
|---|---|---|---|---|
| $w$ | displacement at free end of beam | | $\nu$ | Poisson's ratio |
| $w_{\text{exact}}$ | exact value of displacement | | $\{\sigma\}^{\mathsf{T}}$ | stress vector of $\{\sigma_x\ \sigma_y\ \sigma_z\ \tau_{xy}\ \tau_{yz}\ \tau_{zx}\}$ |
| $[\mathbf{Y}]$ | stress interpolation matrix | | $\sigma_r, \sigma_t$ | radial and tangential stress components |
| $[\mathbf{Z}]$ | $[\mathbf{L}][\mathbf{N}]$ | | $\sigma_x, \sigma_y, \sigma_z$ | normal stress components |
| $z_g$ | $z$-coordinate of Gauss point | | $\tau_{xy}, \tau_{yz}, \tau_{zx}$ | shear stress components |
| $\{\beta_e\}$ | vector of element deformations corresponding to forces $\{\mathbf{F}_e\}$ | | $\Phi_k$ | stress functions |
| | | | $\phi_q$ | linear functions of constants $C_{i,j}^{(k)}$ |

# References

1. Zienkiewicz, O.C.: The Finite Element Method. McGraw-Hill Book Co., New York, 1977.
2. Cook, R.D.: Concepts and Applications of Finite Element Analysis. John Wiley & Sons, New York, 1981.
3. Gallagher, R.H.: Finite Element Analysis: Fundamentals. Prentice-Hall, Inc., Englewood Cliffs, NJ, 1975.
4. Martin, H.C.: Introduction to Matrix Methods of Structural Analysis. McGraw-Hill Book Co., New York, 1966.
5. Robinson, J.: Integrated Theory of Finite Element Methods. John Wiley & Sons, London, 1973.
6. Cassell, A.C.; Henderson, J.C. de C.; and Kaveh, A: Cycle Bases for the Flexibility Analysis of Structures. Comput. Meth. App. Mech. Engng., vol. 8, 1974, pp. 521–528.
7. Kaneko, I.; Lawo, M.; and Thierauf, G.: On Computational Procedures for the Force Method. Int. J. Num. Meth. Engng., vol. 18, 1982, pp. 1469–1495.
8. Spilker, R.L.; Maskeri, S.M.; and Kania, E.: Plane Isoparametric Hybrid-Stress Elements: Invariance and Optimal Sampling. Int. J. Num. Meth. Engng., vol. 17, 1981, pp 1469–1496.
9. Spilker, R.L.; and Singh, S.P.: Three-Dimensional Hybrid-Stress Isoparametric Quadratic Displacement Elements. Int. J. Num. Meth. Engng., vol. 18, 1982, pp. 445–465.
10. Spilker, R.L.: Improved Axisymmetric Hybrid-Stress Elements Including Behavior for Nearly Incompressible Materials. Int. J. Num. Meth. Engng., vol. 17, 1981, pp. 483–501.
11. Spilker, R.L.; and Munir, N.I.: The Hybrid-Stress Model for Thin Plates. Int. J. Num. Meth. Engng., vol. 15, 1980, pp. 1239–1260.
12. Patnaik, S.N.: An Integrated Force Method for Discrete Analysis. Int. J. Num. Meth. Engng., vol. 6, 1973, pp. 237–251.
13. Patnaik, S.N.: The Integrated Force Method Versus the Standard Force Method. Comput. Struct., vol. 22, no. 2, 1986, pp. 151–163.
14. Patnaik, S.N.; Berke, L.; and Gallagher, R.H.: Integrated Force Method Versus Displacement Method for Finite Element Analysis. Comput. Struct., vol. 38, no. 4, 1991, pp. 377–407.
15. Vijayakumar, K.; Murty, A.V. Krishna; and Patnaik, S.N.: A Basis for the Analysis of Solid Continua Using the Integrated Force Method. AIAA J., vol. 26, 1988, pp. 628–629.
16. Patnaik, S.N.; and Joseph, K.T.: Generation of the Compatibility Matrix in the Integrated Force Method.Comput. Meth. App. Mech. Engng., vol. 55, no. 3, 1986, pp. 239–257.
17. Patnaik, S.N.; Berke, L.; and Gallagher, R.H.: Compatibility Conditions of Structural Mechanics for Finite Element Analysis. AIAA J., vol. 29, May 1991, pp. 820–829.
18. Patnaik, S.N.; and Yadagiri, S.: Frequency Analysis of Structures by Integrated Force Method. J. Sound Vib., vol. 83, no. 1, 1982, pp. 93–109.
19. Patnaik, S.N.; and Gallagher, R.H.: Gradients of Behaviour Constraints and Reanalysis Via the Integrated Force Method. Int. J. Num. Meth. Engng., vol. 23, 1986, pp. 2205–2212.
20. Patnaik, S.N.; and Yadagiri, S.: Design for Frequency in the Integrated Force Method. Comput. Meth. App. Mech. Engng., vol. 16, 1978, pp. 213–230.
21. Patnaik, S.N.; Guptill, J.; and Berke, L: Singularity in Structural Optimization. Int. J. Num. Meth. Engng., vol. 36, 1993, pp. 931–944.
22. Patnaik, S.N., et al.: Improved Accuracy for Finite Element Structural Analysis Via a New Integrated Force Method. NASA TP-3204, 1992.
23. Kaljevic, I.; Patnaik, S.N.; and Hopkins, D.A.: Development of Finite Elements for Two-Dimensional Structural Analysis Using the Integrated Force Method. NASA TM-4655, 1995.
24. Pian, T.H.H.; and Chen, D.-P.: Alternative Ways for Formulation of Hybrid Stress Elements. Int. J. Num. Meth. Engng., vol. 18, 1982, pp. 1679–1684.
25. Pian, T.H.H.; and Sumihara, K.: Rational Approach for Assumed Stress Elements. Int. J. Num. Meth. Engng., vol. 20, 1982, pp. 1685–1695.
26. Pian, T.H.H.; Chen, D.-P.; and Kang, D: A New Formulation of Hybrid/ Mixed Finite Element. Comput. Struct., vol. 16, 1983, pp. 81–87.
27. Pian, T.H.H.; and Cheng, D.: On the Suppression of Zero Energy Deformation Modes. Int. J. Num. Meth. Engng., vol. 19, 1983, pp. 1741–1752.
28. Washizu, K.: Variational Methods in Elasticity and Plasticity. Pergamon Press, Oxford, 1968.
29. Keast, P.: Moderate-Degree Tetrahedral Quadrature Formulas. Comput. Meth. App. Mech. Engng., vol. 55, 1986, pp. 339–348.
30. Timoshenko, S.P.; and Goodier, J.N.: Theory of Elasticity. McGraw-Hill Book Co., New York, 1970.
31. Timoshenko, S.P; and Woinowsky-Krieger, S.: Theory of Plates and Shells. McGraw-Hill Book Co., New York, 1959.

# REPORT DOCUMENTATION PAGE

Public reporting burden for this collection of information is estimated to average 1 hour per response, including the time for reviewing instructions, searching existing data sources, gathering and maintaining the data needed, and completing and reviewing the collection of information. Send comments regarding this burden estimate or any other aspect of this collection of information, including suggestions for reducing this burden, to Washington Headquarters Services, Directorate for Information Operations and Reports, 1215 Jefferson Davis Highway, Suite 1204, Arlington, VA 22202-4302, and to the Office of Management and Budget, Paperwork Reduction Project (0704-0188), Washington, DC 20503.

| 1. AGENCY USE ONLY (Leave blank) | 2. REPORT DATE | 3. REPORT TYPE AND DATES COVERED |
|---|---|---|
| | April 1996 | Technical Memorandum |

**4. TITLE AND SUBTITLE**

Element Library for Three-Dimensional Stress Analysis by the Integrated Force Method

**5. FUNDING NUMBERS**

WU–505–63–5B

**6. AUTHOR(S)**

Igor Kaljević, Surya N. Patnaik, and Dale A. Hopkins

**7. PERFORMING ORGANIZATION NAME(S) AND ADDRESS(ES)**

National Aeronautics and Space Administration
Lewis Research Center
Cleveland, Ohio 44135–3191

**8. PERFORMING ORGANIZATION REPORT NUMBER**

E–9522

**9. SPONSORING/MONITORING AGENCY NAME(S) AND ADDRESS(ES)**

National Aeronautics and Space Administration
Washington, DC 20546–0001

**10. SPONSORING/MONITORING AGENCY REPORT NUMBER**

NASA TM–4686

**11. SUPPLEMENTARY NOTES**

Igor Kaljević, Ohio Aerospace Institute, 22800 Cedar Point Road, Cleveland, Ohio 44142; Surya N. Patnaik, Ohio Aerospace Institute, and NASA Resident Research Associate at Lewis Research Center; Dale A. Hopkins, NASA Lewis Research Center. Responsible person, Dale A. Hopkins, organization code 5210, (216) 433–3260.

**12a. DISTRIBUTION/AVAILABILITY STATEMENT**

Unclassified - Unlimited
Subject Category 39

This publication is available from the NASA Center for Aerospace Information, (301) 621–0390.

**12b. DISTRIBUTION CODE**

**13. ABSTRACT (Maximum 200 words)**

The Integrated Force Method, a recently developed method for analyzing structures, is extended in this paper to three-dimensional structural analysis. First, a general formulation is developed to generate the stress interpolation matrix in terms of complete polynomials of the required order. The formulation is based on definitions of the stress tensor components in terms of stress functions. The stress functions are written as complete polynomials and substituted into expressions for stress components. Then elimination of the dependent coefficients leaves the stress components expressed as complete polynomials whose coefficients are defined as generalized independent forces. Such derived components of the stress tensor identically satisfy homogenous Navier equations of equilibrium. The resulting element matrices are invariant with respect to coordinate transformation and are free of spurious zero-energy modes. The formulation provides a rational way to calculate the exact number of independent forces necessary to arrive at an approximation of the required order for complete polynomials. The influence of reducing the number of independent forces on the accuracy of the response is also analyzed. The stress fields derived are used to develop a comprehensive finite element library for three-dimensional structural analysis by the Integrated Force Method. Both tetrahedral- and hexahedral-shaped elements capable of modeling arbitrary geometric configurations are developed. A number of examples with known analytical solutions are solved by using the developments presented herein. The results are in good agreement with the analytical solutions. The responses obtained with the Integrated Force Method are also compared with those generated by the standard displacement method. In most cases, the performance of the Integrated Force Method is better overall.

**14. SUBJECT TERMS**

Integrated Force Method; Three-dimensional analysis; Element library

**15. NUMBER OF PAGES**

25

**16. PRICE CODE**

A03

| 17. SECURITY CLASSIFICATION OF REPORT | 18. SECURITY CLASSIFICATION OF THIS PAGE | 19. SECURITY CLASSIFICATION OF ABSTRACT | 20. LIMITATION OF ABSTRACT |
|---|---|---|---|
| Unclassified | Unclassified | Unclassified | |

NSN 7540-01-280-5500